Hindawi
Oxidative Medicine and Cellular Longevity
Volume 2020, Article ID 4959821, 20 pages
https://doi.org/10.1155/2020/4959821

*Research Article*

# Glucose Starvation-Induced Rapid Death of Nrf1α-Deficient, but Not Nrf2-Deficient, Hepatoma Cells Results from Its Fatal Defects in the Redox Metabolism Reprogramming

**Yu-ping Zhu,[1] Ze Zheng,[1] Yuancai Xiang,[2] and Yiguo Zhang[1]**

[1]*The Laboratory of Cell Biochemistry and Topogenetic Regulation, College of Bioengineering and Faculty of Medical Sciences, Chongqing University, No. 174 Shazheng Street, Shapingba District, Chongqing 400044, China*
[2]*Department of Biochemistry and Molecular Biology, College of Basic Medical Sciences, Southwest Medical University, Sichuan 646000, China*

Correspondence should be addressed to Yiguo Zhang; yiguozhang@cqu.edu.cn

Received 27 February 2020; Revised 8 May 2020; Accepted 29 May 2020; Published 28 July 2020

Academic Editor: Reiko Matsui



Metabolic reprogramming exists in a variety of cancer cells, with the most relevance to glucose as a source of energy and carbon for survival and proliferation. Of note, Nrf1 was shown to be essential for regulating glycolysis pathway, but it is unknown whether it plays a role in cancer metabolic reprogramming, particularly in response to glucose starvation. Herein, we discover that *Nrf1α*$^{-/-}$ hepatoma cells are sensitive to rapid death induced by glucose deprivation, such cell death appears to be rescued by *Nrf2* interference, but HepG2 (wild-type, *WT*) or *Nrf2*$^{-/-}$ cells are roughly unaffected by glucose starvation. Further evidence revealed that *Nrf1α*$^{-/-}$ cell death is resulted from severe oxidative stress arising from aberrant redox metabolism. Strikingly, altered gluconeogenesis pathway was aggravated by glucose starvation of *Nrf1α*$^{-/-}$ cells, as also accompanied by weakened pentose phosphate pathway, dysfunction of serine-to-glutathione synthesis, and accumulation of reactive oxygen species (ROS) and damages, such that the intracellular GSH and NADPH were exhausted. These demonstrate that glucose starvation leads to acute death of *Nrf1α*$^{-/-}$, rather than *Nrf2*$^{-/-}$, cells resulting from its fatal defects in the redox metabolism reprogramming. This is owing to distinct requirements of Nrf1 and Nrf2 for regulating the constructive and inducible expression of key genes involved in redox metabolic reprogramming by glucose deprivation. Altogether, this work substantiates the preventive and therapeutic strategies against *Nrf1α*-deficient cancer by limiting its glucose and energy demands.

## 1. Introduction

Metabolic reprogramming is involved in deregulating anabolism and catabolism of glucose, fatty acids, and amino acids, which is existing in a variety of cancer cells [1], to facilitate those uncontrolled cell growth and proliferation. Usually, cancer cells increase their uptake of nutrients, mainly including glucose and glutamine. Of note, the ensuing metabolism of glucose, as a major nutrient to fuel cell growth and proliferation, comprises glycolysis pathway, gluconeogenesis pathway, pentose phosphate pathway (PPP), and serine synthesis pathway (SSP), all of which occur in the cytoplasm, besides the tricarboxylic acid cycle (i.e., TCA cycle) occurring in the mitochondria [2]. Among these, glycolysis is a central pathway of glucose metabolism but also can be branched towards many anabolic pathways *via* its metabolic intermediates [3]. In cancer cells, decreases in both their oxidative phosphorylation and aerobic glycolysis are accompanied by increases in the another glycolytic flux, which is independent of oxygen concentration to support the enhanced anabolic demands (of e.g., nucleotides, amino acids, and lipids) by providing glycolytic intermediates as raw material [4, 5]. Thereby, such metabolic changes constitute one of the typical hallmarks of tumor cells [1, 6].

Clearly, cell life and death decisions are influenced by its cellular metabolism [7], particularly the metabolism of cancer cells, which is the most relevant to glucose as a source of energy and carbon. A recent study has uncovered the

lower glycolytic rates leading to enhanced cell death by apoptosis [8]. By contrast, the another enforced glycolysis can also effectively inhibit apoptosis [9, 10]. As for the more nutrient uptake than that of normal cells, cancer cells frequently undergo certain metabolic stress due to the shortages in supply of oxygen, nutrients, and growth factors. As such, the rapidly proliferating cancer cells were also unable to stop their anabolic and energy requirements, which eventually leads to cell death [11]. Thereby, such a nutrient limitation has been proposed as an effective approach to inhibit the proliferation of cancer cells. For this end, glucose starvation is also considered as a major form of metabolic stress in cancer cells [12]. However, whether the determination of these cell life-or-death fates is influenced in response to metabolic stress induced by glucose starvation remains to be not well understood.

Glucose metabolism is also regulated by the proto-oncogene c-Myc, which was involved in glycolysis by regulating the glycolytic enzymes [13] and also promoted serine biosynthesis upon nutrient deprivation in cancer cells [14]. The another key oncogene HIF-1 was also identified to act as a central regulator of glucose metabolism [15, 16]. Besides, the tumor suppressor p53 can also play a key negative regulatory role in glycolysis by reducing the glucose uptake [17]. Herein, we determined whether two antioxidant transcription factors Nrf1 (also called Nfe2l1, as a tumor repressor) and Nrf2 (as a tumor promoter) are required for glycolysis and other glucose metabolic pathways and also involved in the redox metabolic reprogramming induced by glucose deprivation.

Among the cap'n'collar (CNC) basic-region leucine zipper (bZIP) family of transcription factor, Nrf1 and Nrf2 are two important members for maintaining redox homeostasis by binding = antioxidant response elements (AREs) of their downstream gene promoters [18]. However, ever-mounting evidence revealed that the water-soluble Nrf2 activation promotes cancer progression and metastasis [19–21]. Notably, Nrf2 also has a direct or another indirect role in all the hallmarks of cancer, such as mediating metabolic reprogramming [22] and altering redox homeostasis [23]. By contrast, the membrane-bound Nrf1 is subjected to alternative translation and proteolytic processing of this CNC-bZIP protein to yield multiple distinct isoforms of between 140 kDa and 25 kDa; they included TCF11/Nrf1$\alpha$ (120~140 kDa), Nrf1$\beta$ (~65 kDa), Nrf1$\gamma$ (~36 kDa), and Nrf1$\delta$ (~25 kDa). Among them, Nrf1$\alpha$ was identified to exist as a major isoform in HepG2 cells as described previously [24]. The specific knockout of Nrf1$\alpha$ (as a dominant tumor repressor) leads to obvious malignant proliferation and tumor metastasis of *Nrf1α*$^{-/-}$-derived hepatoma in xenograft model mice [25]. Besides, Nrf1 was also considered to be involved in hepatic lipid metabolism by directly regulating *Lipin1* and *PGC-1* genes [26]. Moreover, Nrf1 was also found to contribute to the negative regulation of the cystine/glutamate transporter and lipid-metabolizing enzymes [27]. Interestingly, Nrf1 was also positively involved in glycolysis pathway by regulating the *Slc2a2*, *Gck* [28], and *HK1* genes [29]. However, it is not clear about a role of Nrf1 in mediating the cancer cellular response to metabolic stress, especially stimulated by glucose deprivation.

In this study, we observed a surprising change in the growth of *Nrf1α*$^{-/-}$ cells starved in a nonglucose medium. It was found that *Nrf1α*$^{-/-}$ cells were more sensitive to glucose deprivation, leading to acute death within 12 h of glucose deprivation, while both cases of *WT* and *Nrf2*$^{-/-}$ were almost unaffected. As such, the glucose starvation-induced death of *Nrf1α*$^{-/-}$ cells was also rescued by *Nrf2* interference. Further examinations revealed that a large amount of reactive oxygen species (ROS) was accumulated by glucose deprivation in *Nrf1α*$^{-/-}$ cells, leading to severe oxidative stress. Such a redox imbalance was also attributable to the fact that the intracellular reducing agents (i.e., GSH) were exhausted during glucose deprivation. This was due to fatal defects of *Nrf1α*$^{-/-}$ cells, resulting in aberrant expression of some key genes (e.g., *CAT*, *GPX1*, *GSR*, *PCK1/2*, *G6PD*, *PHGDH*, and *ATF4*) that are responsible for the redox metabolism reprogramming of *Nrf1α*$^{-/-}$, but not *Nrf2*$^{-/-}$, cells, albeit these genes were differentially regulated by Nrf1 and/or Nrf2. Collectively, these demonstrate that Nrf1 and Nrf2 play distinct and even opposite roles in mediating cancer cellular responses to the metabolic stress induced by glucose starvation. Notably, Nrf1 acts as a pivotal player to determine the steady-state level of distinct intracellular redox homeostasis.

## 2. Results

*2.1. Nrf1α*$^{-/-}$ *Cells Are Susceptible to the Cellular Death from Glucose Deprivation.* To explore whether both CNC-bZIP factors exert distinct or opposite roles in mediating the cancer cellular response to metabolic stress, *Nrf1α*$^{-/-}$- and *Nrf2*$^{-/-}$-deficient HepG2 cell lines (both had been established by Qiu et al. [30]), along with *WT* cells, were subjected to glucose-free starvation for distinct lengths of time. Subsequently, changes in these cell morphology after glucose deprivation were observed by microscopy. Within 6 h of glucose starvation, no obvious abnormalities of all three cell lines were shown (Figure S1A). In fact, they were growing well, with no changes in the small number of dead cells (Figure S1B). However, when the time of glucose starvation was extended to 12 h, *Nrf1α*$^{-/-}$ cells displayed apparent morphological characteristics of cell death (resembling the necrosis and/or necroptosis, Figure 1(a)), of which such dead cells were stained by trypan blue to 49.26% (Figure 1(b)). By sharp contrast, both *WT* and *Nrf2*$^{-/-}$ cell lines were largely unaffected by 12 h of glucose starvation (Figures 1(a) and 1(b)). These cell death or survival was further corroborated by flow cytometry analysis of dual staining cells with fluorescent Annexin V and propidium iodide (PI), showing that *Nrf1α*$^{-/-}$ cells were more susceptible to the cell death induced by glucose deprivation for 12 h, when compared with other two examined cell lines of *WT* and *Nrf2*$^{-/-}$ (Figure 1(c)).

As the glucose starvation was further extended to 24 h, almost all *Nrf1α*$^{-/-}$ cells were subjected to the cellular death (Figure S1C). Such prolonged glucose starvation-induced death of *Nrf1α*$^{-/-}$ cells was incremented to 95.6% of their examined cells, but only a small number (20%) of *WT* cells were showed to its cellular death (Figure S1D). Meanwhile, *Nrf2*$^{-/-}$ cells appeared to be remaining robust resistant to the

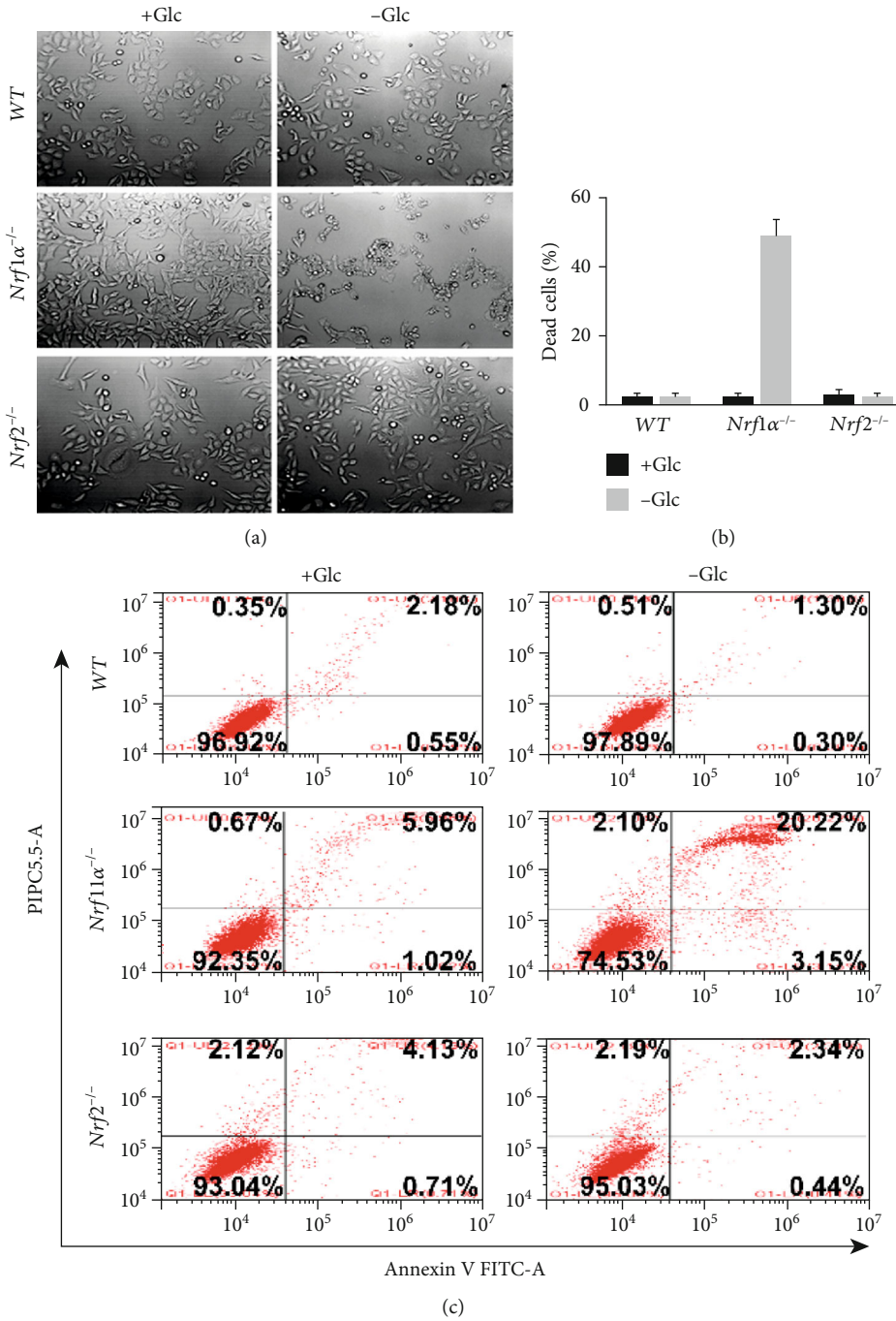


Figure 1: Continued.

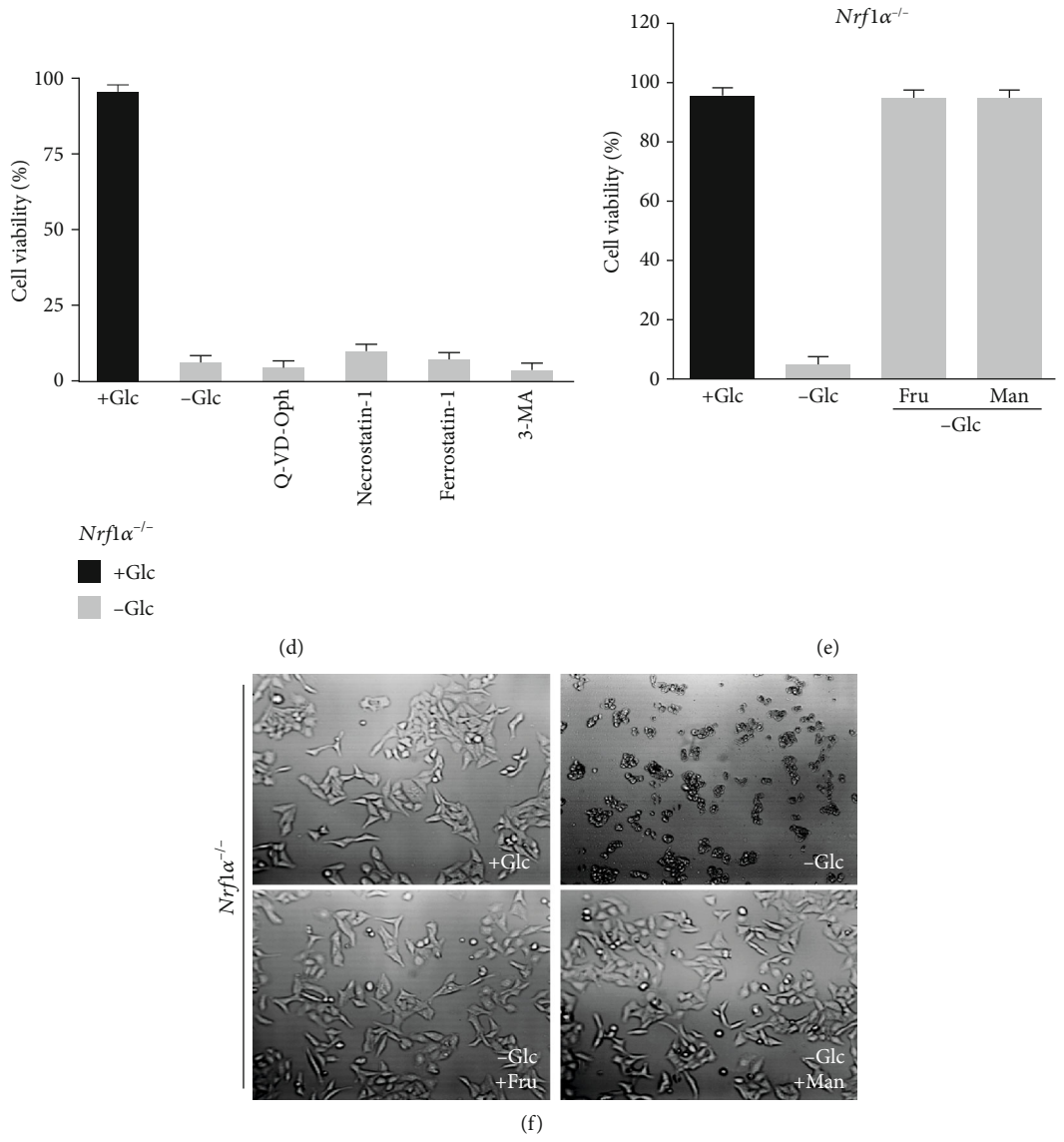


Figure 1: The response of *Nrf1α*$^{-/-}$ cells to glucose starvation. (a) Morphological changes of *WT*, *Nrf1α*$^{-/-}$, and *Nrf2*$^{-/-}$ cells, which had been subjected to glucose deprivation for 12 h, were observed by microscopy (with an original magnification of 200x). (b) The percentage of their dead cells was calculated after being stained by trypan blue. (c) The apoptosis of glucose-starved cells was analyzed by flow cytometry, after being incubated with Annexin V-FITC and PI. (d) *Nrf1α*$^{-/-}$ cell viability was determined by incubation for 24 h with q-VD-OPH (10 $\mu$M), Necrostatin-1 (100 $\mu$M), Ferrostatin-1 (2 $\mu$M), or 3-methyladenine (2 mM) in the glucose-free media, each of which was resolved in DMSO as a vehicle. (e) *Nrf1α*$^{-/-}$ cell survival was recovered from glucose deprivation by being cultured for 24 h in alternative media containing 25 mM of fructose (Fru) or mannose (Man). (f) Morphology of Fru/Man-recovered *Nrf1α*$^{-/-}$ cells was visualized by microscopy (with an original magnification of 200x).

putative cellular death stimulated by glucose deprivation for 24 h, however (Figure S1, C & D).

Next, several inhibitors of distinct signaling pathways towards cell death were here employed so as to determine which types of *Nrf1α*$^{-/-}$ cell death are resulted from glucose deprivation. Unexpectedly, treatment of *Nrf1α*$^{-/-}$ cells with Q-VD-OPH (acting as a pan-caspase inhibitor to block the apoptosis pathway), Necrostatin-1 (as a necroptosis inhibitor), Ferrostatin-1 (as a ferroptosis inhibitor), and 3-methyladenine (3-MA, as an autophagy inhibitor) demonstrated that they all had not exerted any cytoprotective effects against the cellular death caused by glucose deprivation (Figure 1(d)). Thereby, it is inferable that *Nrf1α*$^{-/-}$ cell death from glucose withdrawal may pertain to a major nonapoptotic form of cellular necrosis, but the detailed mechanism of *Nrf1α*$^{-/-}$ cell death awaits further study.

Since glucose deprivation, but not the glycolytic inhibition, leads to death of *Nrf1α*$^{-/-}$ cells, we hence investigated whether the cellular death was rescued by other sugar sources, such as fructose or mannose, because both could also serve as a potent alternative to glucose. As shown in Figures 1(e) and 1(f), the results unraveled that fructose and mannose were metabolically utilized in *Nrf1α*$^{-/-}$ cells insomuch as to resist against the cell death induced by glucose deprivation. This

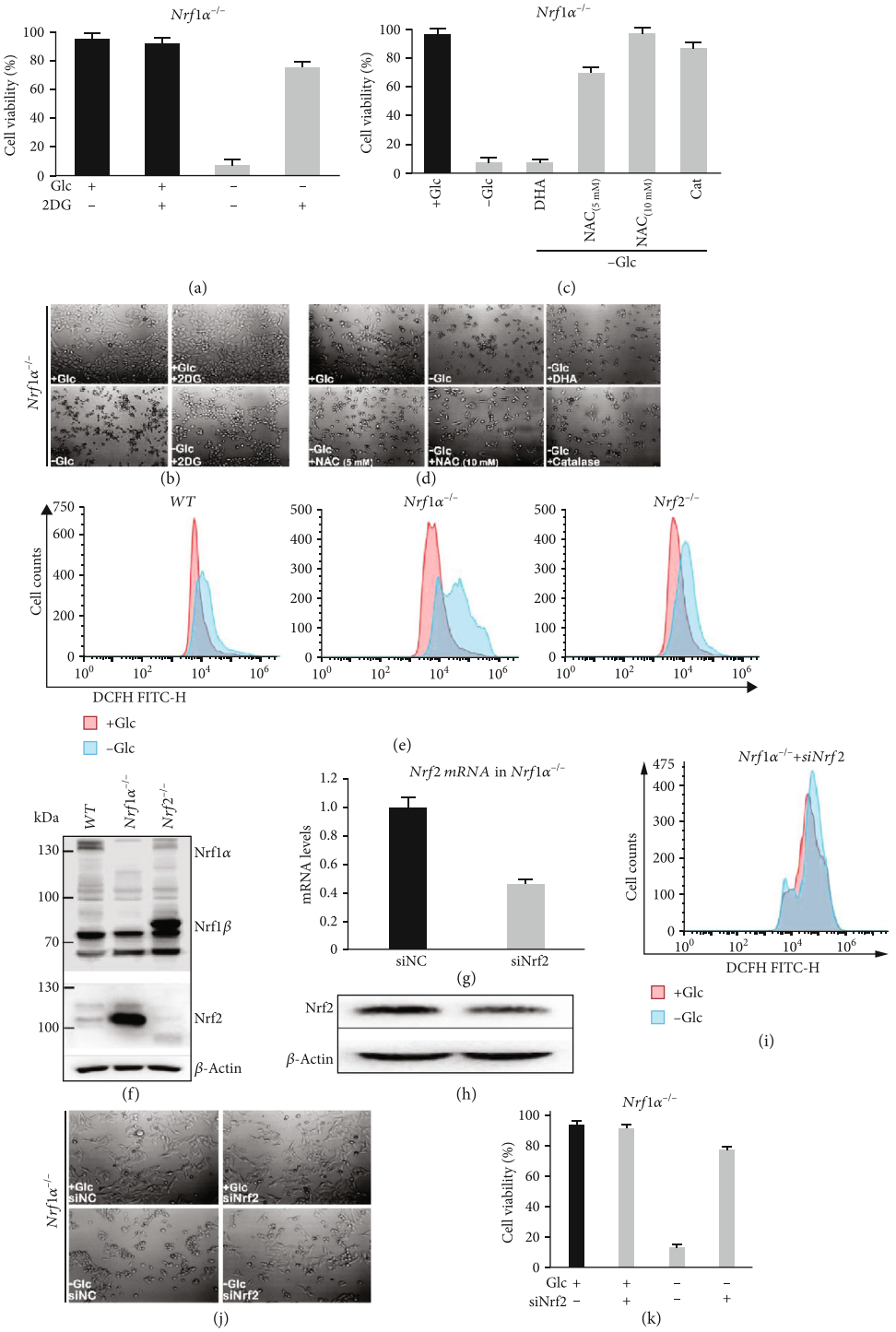


FIGURE 2: Distinct redox states of starved or rescued *Nrf1α*$^{-/-}$ cells with different morphological changes. (a) *Nrf1α*$^{-/-}$ cells had been rescued by incubation for 24 h with 2-deoxyglucose (2DG, 10 mM in the glucose-free media), before the cell viability was determined by trypan blue staining. (b) Morphology of 2DG-rescued *Nrf1α*$^{-/-}$ cells was visualized by microscopy (with an original magnification of 200x). (c) *Nrf1α*$^{-/-}$ cell viability was calculated after they had been cultured for 24 h in glucose-free media containing N-acetyl-cysteine (NAC at 5-10 mM), catalase (CAT at 50 units/ml), or dehydroascorbic acid (DHA at 100 $\mu$M). (d) Morphological changes of *Nrf1α*$^{-/-}$ cells, which had been treated with NAC, CAT or DHA, were observed by microscopy (with an original magnification of 200x). (e) Distinct ROS levels were determined by flow cytometry analysis of *WT*, *Nrf1α*$^{-/-}$, and *Nrf2*$^{-/-}$ cells that had been starved, or not starved, for 12 h. (f) Abundances of Nrf1 and Nrf2 proteins were determined by Western blotting of *WT*, *Nrf1α*$^{-/-}$, and *Nrf2*$^{-/-}$ cells. (g, h) The interference of *siNrf2* in *Nrf1α*$^{-/-}$ cells was identified by RT-qPCR (g) and Western blotting (h). (i) Changes in ROS levels of *Nrf1α*$^{-/-}$*+siNrf2* cells were analyzed by flow cytometry after 12 h of glucose deprivation. (j) The effects of *siNrf2* on glucose-starved cell morphology were observed by microscopy (with an original magnification of 200x). (k) *Nrf1α*$^{-/-}$*+siNrf2* cell viability was evaluated after they had been subjected to glucose starvation for 24 h.

demonstrates that the lack of sugar source is responsible for determining the death fate of *Nrf1α*$^{-/-}$ cells.

*2.2. Nrf1α*$^{-/-}$ *Cell Death Is Driven by Glucose Deprivation Leading to Severe Endogenous Oxidative Stress.* Clearly, cell life or death fate decisions are selectively determined by the intracellular energy metabolism and redox homeostasis [31]. Thereby, we herein examined whether endogenous oxidative stress of *Nrf1α*$^{-/-}$ cells is stimulated by glucose starvation contributing to the cellular responsiveness to death. As anticipated, Figures 2(a) and 2(b)) showed that *Nrf1α*$^{-/-}$ cell death arising from the removal of glucose enabled to be sufficiently rescued after addition of 2-deoxyglucose (2DG, as an analogue of glucose) to the sugar-free culture medium. This is due to the fact that 2DG has a potent ability to inhibit the glycolysis, and thus this treatment of *Nrf1α*$^{-/-}$ cells enabled the existing available glucose to enter the PPP route in order to generate certain amounts of NADPH (that acts as a major metabolically reducing agent required for the setting of intracellular basal redox state [32]).

Further examinations revealed that glucose starvation-induced death of *Nrf1α*$^{-/-}$ cells was significantly mitigated or completely rescued by treatment with N-acetyl-L-cysteine (NAC, an antioxidant agent to increase glutathione synthesis) or catalase (CAT, an enzyme that catalyzes the breakdown of hydrogen peroxide) (Figures 2(c) and 2(d)). By contrast, *Nrf1α*$^{-/-}$ cell death triggered by glucose starvation was almost unaffected by treatment with dehydroascorbic acid (DHA, as a stable oxidative product of L-ascorbic acid). These suggest that severe oxidative stress may contribute to the rapid death of *Nrf1α*$^{-/-}$ cells from glucose deprivation. This notion is further evidenced by flow cytometry analysis of distinct cellular oxidative states (Figure 2(e)). The results unraveled that glucose deprivation caused an obvious accumulation of ROS in *Nrf1α*$^{-/-}$ cells, with the oxidative fluorescent images becoming widened and right-shifted, when compared with the other two cases of *WT* and *Nrf2*$^{-/-}$ (only with modestly increased ROS levels) (Figure 2(e)). Collectively, these imply a fatal defect of *Nrf1α*$^{-/-}$, rather than *Nrf2*$^{-/-}$, cells in the antioxidant cytoprotective response against the cellular death attack from glucose withdrawal stress.

*2.3. Rapid Death of Glucose-Starved Nrf1α*$^{-/-}$ *Cells Can Be Rescued by Interference with Nrf2.* Based on a similar structure and function of Nrf1 and Nrf2 [33], it is postulated that the loss of Nrf1*α* is likely compensated by Nrf2. As anticipated, Western blotting revealed that aberrant high expression of Nrf2 was determined in *Nrf1α*$^{-/-}$ cells, when compared with that of *WT* cells (Figure 2(f)); this is consistent with our previous finding by Qiu et al. [30] (in which subcellular distribution of Nrf2 in *Nrf1α*$^{-/-}$ cells was shown). Conversely, considerable lower expression levels of Nrf1*α*-derived protein isoforms were maintained in *Nrf2*$^{-/-}$ cells, albeit with a compensatory higher expression of the short Nrf1*β* (Figure 2(f)).

Since such hyperexpression of Nrf2 in *Nrf1α*$^{-/-}$ cells serves as a complement to *Nrf1α* knockout, it is thus inferable that Nrf2 may also contribute to mediating a putative response of *Nrf1α*$^{-/-}$ cells to death attack by glucose starvation. Thereby, we here tried to interfere with the *Nrf2* expression by siRNA transfection into glucose-starved *Nrf1α*$^{-/-}$ cells. As shown in Figures 2(g) and 2(h)), both mRNA and protein expression levels of Nrf2 were significantly knocked down by its specific siRNA (i.e., *siNrf2*) in *Nrf1α*$^{-/-}$ cells. More interestingly, glucose starvation-induced death of *Nrf1α*$^{-/-}$ cells was strikingly ameliorated by the interference of *siNrf2* (Figures 2(j) and 2(k)). This is also substantiated by further evidence obtained from flow cytometry analysis of the cell death (Figure S1E). Such effectively *siNrf2*-alleviated death of *Nrf1α*$^{-/-}$ cells was accompanied by a significant reduction in the intracellular ROS accumulation by glucose deprivation (Figure 2(i)). Together, these demonstrate that hyperactive Nrf2 can also make a major contribution to the accumulation of ROS products in *Nrf1α*$^{-/-}$ cells, leading to the cellular death driven by glucose starvation.

*2.4. The Failure of Redox Defense Systems in Nrf1α*$^{-/-}$ *Cells Contributes to Its Lethality of Glucose Starvation.* The aforementioned evidence (as shown in Figures 2(c) and 2(e)) demonstrated that glucose starvation-induced death of *Nrf1α*$^{-/-}$ cells resulting from severe oxidative stress was effectively prevented by NAC and CAT. This suggests that the intracellular redox state is rebalanced by either NAC or CAT, because NAC facilitates the conversion of oxidized glutathione (GSSG) to reduced glutathione (GSH) by glutathione(-disulfide) reductase (GR or GSR), while CAT can catalyze hydrogen peroxide ($H_2O_2$) breakdown to water and oxygen, such that the cytotoxic effects of ROS on *Nrf1α*$^{-/-}$ cells are inhibited.

Herein, we further examined changes in basal and glucose starvation-inducible expression of CAT and GSR, as well as other redox cycling and relevant enzymes, including GPX1, PRX1, TRX1, TRX2, NOX4, SOD1, and SOD2 (Figure 3(a)), in *Nrf1α*$^{-/-}$ cells cultured in complete or glucose-free media. As shown in Figures 3(b) and 3(c), RT-qPCR analysis of *Nrf1α*$^{-/-}$ cells demonstrated significant increases in basal mRNA expression levels of *CAT* and *GPX1* (glutathione peroxidase 1, which catalyzes the reduction of $H_2O_2$ and organic hydroperoxides by GSH, so as to protect cells against oxidative damages), when compared with those of *WT* cells. After glucose withdrawal from the culture of *Nrf1α*$^{-/-}$ cells, such basal expression of both *CAT* and *GPX1* was abruptly inhibited close to the levels measured from *WT* cells (Besides GLUT1, other key metabolic enzymes). Similar marked changes in CAT and GPX1 expression were, however, not observed in *Nrf2*$^{-/-}$ cells.

By contrast, basal *GSR* expression was downregulated in *Nrf1α*$^{-/-}$ cells, and glucose deprivation also caused it to be further repressed to a considerable lower level, by comparison to the *WT* cells (Figure 3(d)). However, similar downregulation of *GSR* in *Nrf2*$^{-/-}$ cells was almost unaffected by glucose starvation. Conversely, expression of *PRX1* (peroxiredoxin-1, also called thioredoxin peroxidase 1) was significantly diminished by glucose deprivation in *Nrf2*$^{-/-}$, rather than *Nrf1α*$^{-/-}$, cells, albeit its basal expression was similarly downregulated in these two deficient cell lines (Figure 3(e)). Further examinations of *Nrf1α*$^{-/-}$ and *Nrf2*$^{-/-}$ cells revealed that glucose starvation caused remarkable decreases in expression of TRX1

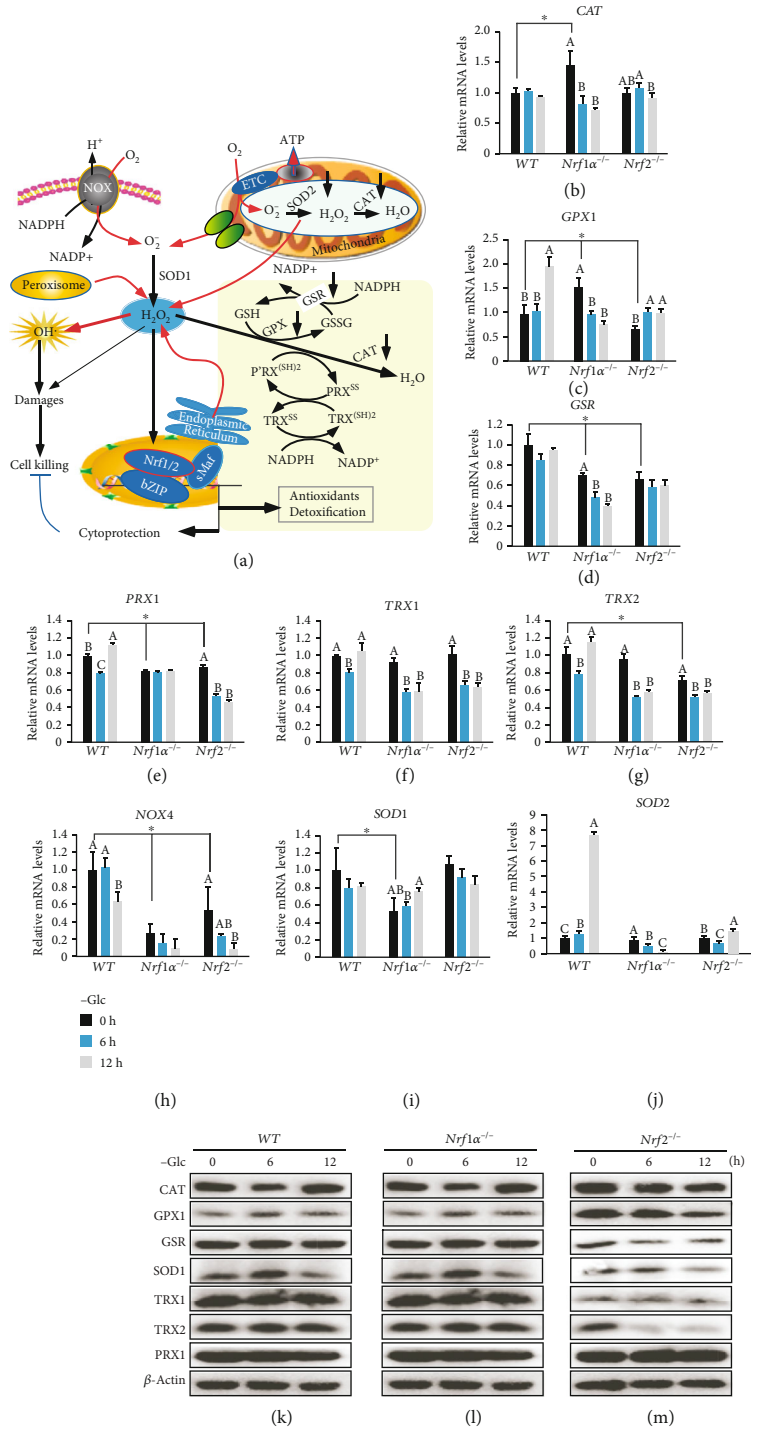


Figure 3: Dysfunction of redox signaling controls and defense systems in glucose-starved *Nrf1α*$^{-/-}$ cells. (a) Schematic representation of intracellular ROS products, along with redox signaling controls and antioxidant defense systems. In this response, Nrf1 and Nrf2 can be induced to translocate the nucleus, in which its functional heterodimer with sMaf or other bZIP proteins is formed in order to transcriptionally regulate distinct subsets of ARE-driven genes, which are responsible for antioxidant, detoxification, and cytoprotection against a variety of cellular stress. (b–j) Alterations in mRNA expression levels of distinct genes, such as (b) *GSR* (glutathione disulfide reductase), (c) *CAT* (catalase), (d) *GPX1* (glutathione peroxidase 1), (e) *PRX1* (peroxidase 1), (f) *TRX1* (thioredoxin 1), (g) *TRX2* (thioredoxin 2), (h) *NOX4* (NADPH oxidase 4), (i) *SOD1* (superoxide dismutase 1), and (j) *SOD2* (superoxide dismutase 2), in *WT*, *Nrf1α*$^{-/-}$, and *Nrf2*$^{-/-}$ cells, which had been or had not been starved in glucose-free media for 0-12 h, were determined by RT-qPCR analysis. Then, the asterisk "∗" only represents a significant change in *WT*, *Nrf1α*$^{-/-}$, and *Nrf2*$^{-/-}$ cell lines in the glucose-free culture for 0 h ($P < 0.05$), while the letters A, B, and C represent significant changes in the same cell line without glucose cultured for 0, 6, and 12 h ($P < 0.05$). (k–m) Changes in abundances of the following proteins CAT, GPX1, GSR, SOD1, TRX1, TRX2, and PRX1 were visualized by Western blotting of *WT* (*k*), *Nrf1α*$^{-/-}$ (l), and *Nrf2*$^{-/-}$ (m) cells that had been or had not been glucose-starved for 0-12 h.

and TRX2 (i.e., both thioredoxin proteins involved in many reversible redox reactions) (Figures 3(f) and 3(g)). In addition, it is intriguing that deficiency of either *Nrf1α* or *Nrf2* also led to significantly decreased expression of *NOX4* (NADPH oxidase 4, which acts as an oxygen sensor and also catalyzes the reduction of molecular oxygen to various ROS) (Figure 3(h)), but the expression of *SOD1* (superoxide dismutase 1) was only significantly decreased in *Nrf1α*$^{-/-}$ cells, while the expression of *SOD2* is hardly affected by *Nrf1α* or *Nrf2* deficiency (Figures 3(i) and 3(j)). Notably, only *WT* cells, but not *Nrf1α*$^{-/-}$ or *Nrf2*$^{-/-}$ cells, showed significant increases in glucose starvation-stimulated expression of *GPX1* and *SOD2* (Figures 3(c) and 3(j)), but not other examined gene transcripts.

Further Western blotting of *Nrf1α*$^{-/-}$ cells unraveled that the expression of CAT, GPX1, GSR, TRX1, and TRX2, but not PRX1 or SOD1, was substantially decreased by glucose deprivation for 12 h (Figures 3(l) and S2B). By contrast, abundances of these examined proteins except PRX1 were only marginally decreased to lesser extents by glucose starvation of *Nrf2*$^{-/-}$ cells (Figures 3(m) and S2C). Such minor effects cannot also be excluded to be attributable to a modest decrease of Nrf1α in Nrf2- deficient cells (Figure 2(f)). In addition, it should be noted that not any increases of the redox-relevant proteins were stimulated by glucose starvation for 6 h to 12 h, even in *WT* cells (Figures 3(k) and S2A). Together, it is postulated that *Nrf1α*$^{-/-}$, but not *Nrf2*$^{-/-}$, cells are likely to have certain fatal defects in setting the intracellular redox homeostasis along with antioxidant defense systems, such that the resulting redox imbalance contributes to severe endogenous oxidative stress and concomitant damages leading to *Nrf1α*$^{-/-}$ cell death, particularly after 12-h glucose starvation.

*2.5. Deregulated Glucose Metabolism and Energy Demands of Nrf1α*$^{-/-}$ *Cells Are Deteriorated by Glucose Deprivation.* Since aerobic glycolysis provides the main energy for cancer cells (as illustrated in Figure 4(a)), it is evitable that the intracellular production of ATP as a major energy source could thus be affected by glucose withdrawal from *WT*, *Nrf1α*$^{-/-}$, and *Nrf2*$^{-/-}$ cell culture in sugar-free media. As shown in Figure 4(b), a substantial diminishment in the basal ATP levels of *Nrf2*$^{-/-}$ cells was determined, and even glucose deprivation-stimulated ATP products were also maintained to considerable lower levels, when compared to those corresponding values measured from *WT* cells. By sharp contrast, the basal ATP levels of *Nrf1α*$^{-/-}$ cells (with aberrant hyper-active Nrf2) were significantly elevated (Figure 4(b)), so as to meet the needs of its malignant growth and proliferation [25, 30]). Intriguingly, such higher ATP production by *Nrf1α*$^{-/-}$ cells was further promoted by glucose starvation for 6 h, and thereafter abruptly declined by 12-h prolonged starvation to basal levels of wild-type cells (Figure 4(b)). Accordingly, similar alternations in basal and glucose starvation-stimulated expression of *GLUT1* (glucose transporter 1) were also determined in *Nrf1α*$^{-/-}$ cells (Figure 4(c)), so as to meet its highly metabolizable energy requirements. This is further supported by Western blotting of *Nrf1α*$^{-/-}$ cells, displaying a high expression pattern of GLUT1, particularly during glucose-free conditions (Figure 4(o)). Meanwhile, almost unaltered expression of GLUT1 in *Nrf2*$^{-/-}$ cells was observed, even upon glucose starvation (Figure 4(p)). But, this transporter abundances in *WT* cells were modestly decreased after glucose deprivation (Figure 4(n)).

Besides GLUT1, other key metabolic enzymes (e.g., HK1/2, PFKL, and LDHA) required for the glycolysis pathway of cancer cells were also investigated herein. Among them, only hexokinase 2 (HK2) was transcriptionally activated by glucose starvation of *WT* cells, but not of *Nrf1α*$^{-/-}$ or *Nrf2*$^{-/-}$ cells. Although basal mRNA expression of *HK2* was obviously upregulated, but rather its glucose starvation-stimulated expression was significantly suppressed, in *Nrf1α*$^{-/-}$ or *Nrf2*$^{-/-}$ cells (Figure 4(e)). Similarly, a substantial increase in basal *HK1* expression occurred in *Nrf1α*$^{-/-}$ cells, whereas its transcriptional expression was strikingly reduced by glucose deprivation. By contrast, *Nrf2*$^{-/-}$ cells also showed a considerable high level of basal *HK1* expression, albeit its mRNA transcription was unaffected by glucose starvation (Figure 4(d)). Further examinations by Western blotting revealed that both HK1 and HK2 protein expression levels were modestly decreased by glucose starvation of *Nrf1α*$^{-/-}$ cells, but appeared to be unaffected in glucose-starved *WT* and *Nrf2*$^{-/-}$ cells (Figures 4(n)–4(p) and S2, D-F). Moreover, apparent decreases in basal *PFKL* (phosphofructokinase, liver type) and *LDHA* (lactate dehydrogenase A) expression levels were observed in *Nrf1α*$^{-/-}$ cells (Figures 4(f) and 4(g)), of which the latter *LDHA* expression was further decreased by glucose starvation, while *PFKL* was only slightly reduced by this stimulation. Contrarily, *Nrf2*$^{-/-}$ cells showed a substantial increment in basal *PFKL* expression, but its mRNA transcription expression was markedly suppressed upon glucose deprivation (Figure 4(f)). By comparison, a modest decrease in basal expression of *LDHA* was also observed in *Nrf2*$^{-/-}$ cells, but its expression was roughly unaffected (Figure 4(g)). These collective data demonstrate distinct roles of Nrf1 and Nrf2 in controlling the expression of those key genes responsible for glycolysis.

Since the above observation (Figures 2(a) and 2(b)) uncovered that glucose-starved *Nrf1α*$^{-/-}$ cell death was rescued by 2DG, this glucose analogue could render the metabolic flow to enter the PPP and promote NADPH production. As anticipated, RT-qPCR analysis of the rate-limiting enzymes of the PPP showed that mRNA expression levels of *G6PD* (glucose-6-phosphate dehydrogenase) and *PGD* (phosphogluconate dehydrogenase) were significantly decreased after glucose deprivation of *WT*, *Nrf1α*$^{-/-}$, and *Nrf2*$^{-/-}$ cells (Figures 4(h) and 4(i)), albeit bidirectionally positive and negative regulation of their basal expression by *Nrf1α*$^{-/-}$ or *Nrf2*$^{-/-}$ was determined. Furtherly, Western blotting also unraveled that G6PD protein abundances were significantly decreased in glucose-starved *Nrf1α*$^{-/-}$, rather than *WT* and *Nrf2*$^{-/-}$, cell lines (Figures 4(n)–4(p) and S2, D-F).

From the aforementioned evidence, it is postulated that the gluconeogenesis pathway should be enhanced after glucose deprivation, so that the resulting products were allowed to enter the PPP and other (redox) metabolic pathways. Thus, we investigated the expression of certain key enzymes involved in the gluconeogenesis. As shown in Figure 4(k), a significant increment in transcriptional expression of *PCK2*

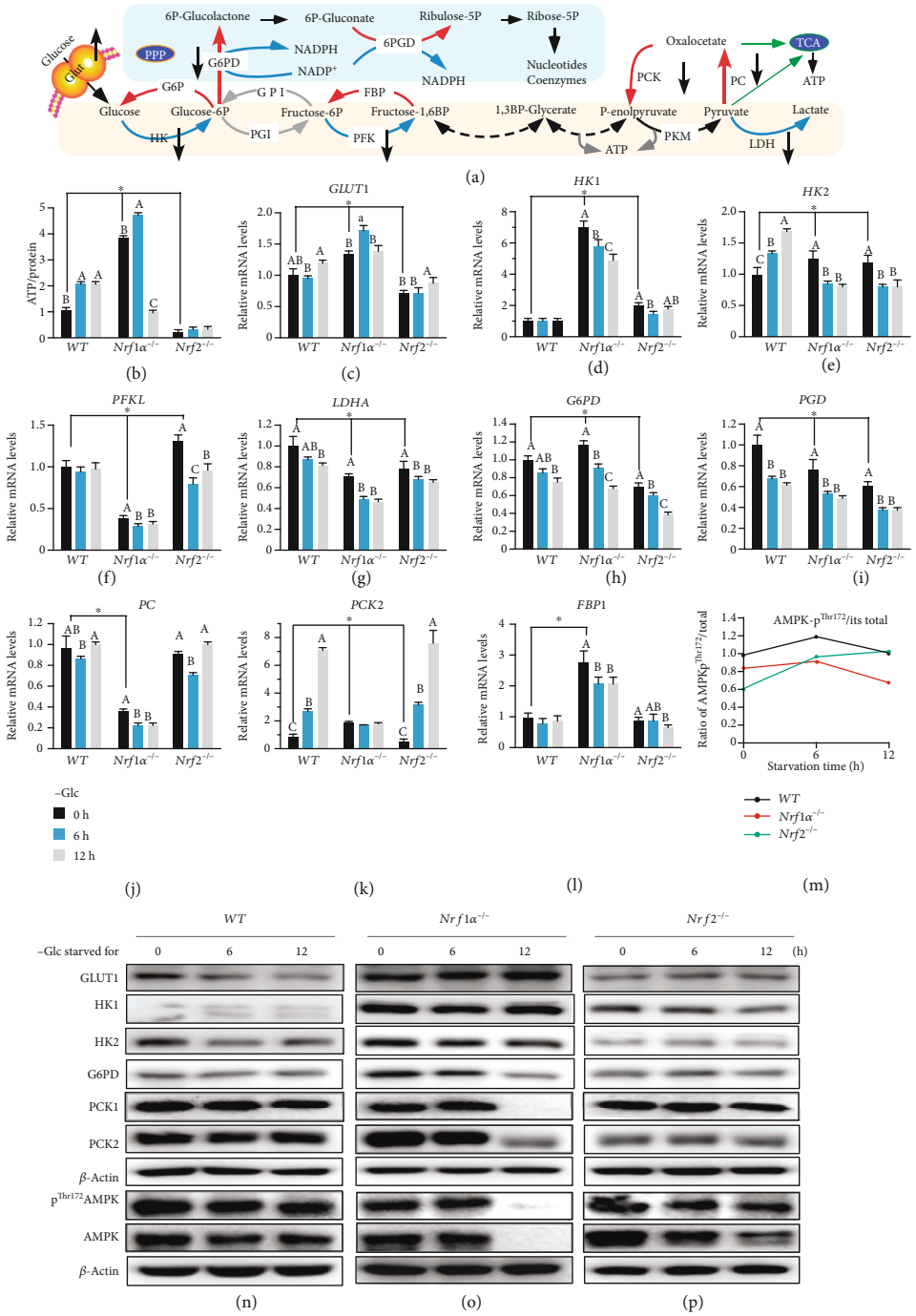


FIGURE 4: Deterioration of altered glucose metabolism and energy demands by glucose deprivation of *Nrf1α*$^{-/-}$ cells. (a) A schematic diagram to give a concise explanation of glycosis, gluconeogenesis, and pentose phosphate pathways (PPP). The key rate-limiting enzymes are indicated, apart from TCA (citric acid cycle). In some words, phospho- is represented by a single *P* letter. (b) Distinct ATP levels of *WT*, *Nrf1α*$^{-/-}$, and *Nrf2*$^{-/-}$ cells were determined after glucose deprivation for 0-12 h. (c–l) Altered mRNA expression levels of key metabolic genes: (i) (c) *GLUT1* (glucose transporter 1), (d) *HK1* (hexokinase 1), (e) *HK2*, (f) *PFKL* (phosphofructokinase liver type), and (g) *LDHA* (lactate dehydrogenase A) involved in the glycolysis pathway; (ii) (h) *G6PD* (glucose-6-phosphate dehydrogenase) and (i) *PGD* (phosphogluconate dehydrogenase) as rate-limiting enzymes in the PPP; (iii) (j) *PC* (pyruvate carboxylase), (k) *PCK2* (phosphoenolpyruvate carboxykinase 2), and (l) *FBP1* (fructose bisphosphatase 1) responsible for the gluconeogenesis pathway, were analyzed by RT-qPCR analysis of *WT*, *Nrf1α*$^{-/-}$, and *Nrf2*$^{-/-}$ cells that had been starved, or not starved, in the glucose-free media for 0-12 h. Then, the asterisk "∗" only represents a significant change in *WT*, *Nrf1α*$^{-/-}$, and *Nrf2*$^{-/-}$ cell lines in the glucose-free culture for 0 h ($P < 0.05$), while the letters A, B, and C represent significant changes in the same cell line without glucose cultured for 0, 6, and 12 h ($P < 0.05$). (m) Phospho-AMPK$^{Thr172}$/AMPK ratios were calculated by the intensity of their immunoblots in *Nrf1/2*$^{+/+}$, *Nrf1α*$^{-/-}$, and *Nrf2*$^{-/-}$ cells. (n–p) Changes in protein abundances of GLUT1, HK1, HK2, G6PD, PCK1, PCK2, AMPK, and its phospho-AMPK$^{Thr172}$ were determined by Western blotting of *Nrf1/2*$^{+/+}$ (n), *Nrf1α*$^{-/-}$ (o), and *Nrf2*$^{-/-}$ (p) cells, after having been glucose-starved, or not, for 0-12 h.

(phosphoenolpyruvate carboxykinase 2) in *WT* and *Nrf2*$^{-/-}$ cells was stimulated by glucose starvation for 6 h to 12 h. However, no changes in mRNA expression of *PCK2* were detected in glucose-starved *Nrf1α*$^{-/-}$ cells, although its basal expression was upregulated (Figure 4(k)). This is further supported by Western blotting of PCK1 and PCK2, revealing that both protein abundances were significantly decreased by glucose starvation, especially for 12 h, in *Nrf1α*$^{-/-}$ cells, but rather almost unaffected in glucose-starved *WT* and *Nrf2*$^{-/-}$ cells (Figures 4(n)–4(p) and S2, D-F). Further examinations of *PC* (pyruvate carboxylase) and *FBP1* (fructose-bisphosphatase 1) unraveled that their mRNA levels were markedly reduced by glucose deprivation in *Nrf1α*$^{-/-}$ cells, but largely unaltered in glucose-starved *WT* or *Nrf2*$^{-/-}$ cell lines (Figures 4(j) and 4(l)). In addition, it should be noted that *Nrf1α*$^{-/-}$ cells manifested downregulation of basal *PC* expression, along with upregulation of basal *FBP1* expression.

Next, we examined changes in active phosphorylation of AMPK (AMP-activated protein kinase), since it acts as a key regulator of energy metabolism [34]. As illustrated in Figure 4(m), the ratio of phosphorylated AMPK$^{Thr172}$ to total protein (as calculated by stoichiometry of their immunoblots as shown in Figures 4(n)–4(p)) was increased by glucose withdrawal from *Nrf2*$^{-/-}$ cells, but conversely decreased in glucose-starved *Nrf1α*$^{-/-}$ cells. The latter notion was also further supported by the fact that almost all of total AMPK and its phospho-AMPK$^{Thr172}$ proteins were evidently abolished by 12-h glucose starvation of *Nrf1α*$^{-/-}$ cells (Figure 4(o)), besides their significant reduction in glucose-starved *Nrf2*$^{-/-}$ cells (Figure 4(p)). Overall, the inactivation of cellular energy switch, along with blockage of its gluconeogenesis and ablation of both its PPP and glycolysis, is inferable as a crucial determinant of *Nrf1α*$^{-/-}$ cell death, resulting from glucose deprivation to deteriorate its altered energy metabolic demands.

*2.6. Upregulation of Serine-to-Glutathione Synthesis by Glucose Deprivation Is Fatally Abolished in Nrf1α*$^{-/-}$ *Cells, Leading to Severe Endogenous Oxidative Stress.* As illustrated in Figure 5(a), *de novo* serine synthesis from glycolytic metabolite 3-phosphoglycerate (3PG) by SSP contributes to major carbons for glutathione biosynthesis and also provides precursors for purine and pyrimidine biosynthetic pathway *via* the folate cycle. In the successive biochemical course, 3PG, as a key intermediate of glycolytic pathway, is allowed to flow into the SSP and thus limit ATP production, while oxidation of 3PG converts $NAD^+$ to NADH so as to affect intracellular redox state. As a result, serine can also be converted to cysteine and glycine by key enzymes (Figure 4(a)), for maintaining intracellular glutathione homeostasis. Therefore, we herein investigated the putative effects of glucose deprivation on serine-to-glutathione synthesis pathways.

As expected, significant increases in mRNA expression of those rate-limiting enzymes, such as *PHGDH* (phospho-glycerate dehydrogenase), *PSAT1* (phosphoserine aminotransferase 1), and *PSPH* (phosphoserine phosphatase), required in the SSP, as well as their upstream regulatory factor *ATF4* (activating transcription factor 4) [35], were triggered by glucose deprivation in *WT* and *Nrf2*$^{-/-}$ cells (Figures 5(b)–5(e)). By contrast, transcriptional induction of *PHGDH*, *PSAT1*, *PSPH*, and *ATF4* by glucose deprivation was completely blocked or suppressed to lesser extents in starved *Nrf1α*$^{-/-}$ cells, albeit with an exception of evident increases in their basal mRNA expression upregulated by loss of *Nrf1α* (Figures 5(b)–5(e)). Accordingly, Western blotting showed that glucose starvation of *WT* cells for 12 h led to modest increases in abundances of PHGDH and PSAT1, rather than ATF4, to greater extents (Figures 5(m) and S2G). However, all three protein expression levels were strikingly decreased by glucose deprivation in *Nrf1α*$^{-/-}$ cells, but unaltered in glucose-starved *Nrf2*$^{-/-}$ cells (Figures 5(n) and 5(o) and S2, H & I).

Further insights into cysteine metabolism by transsulfuarion enzymes, such as CBS (cystathionine $\beta$-synthase) and CTH (cystathionine $\gamma$-lyase), revealed that both were transcriptionally upregulated by glucose starvation in *WT* cells (Figures 5(f) and 5(g)). Similarly, *Nrf2*$^{-/-}$ cells also manifested modest induction of *CBS* and *CTH* by glucose deprivation, notwithstanding the downregulation of their basal expression by loss of Nrf2 (Figures 5(f) and 5(g)). Conversely, the upregulation of basal *CBS* and *CTH* expression occurred in *Nrf1α*$^{-/-}$ cells (with hyper-active Nrf2). However, glucose starvation triggered opposite effects on transcriptional expression of *CBS* and *CTH* in *Nrf1α*$^{-/-}$ cells; the former *CBS* mRNA levels were evidently suppressed, while the latter *CTH* mRNA expression was marginally induced (Figures 5(f) and 5(g)). In addition, glucose deprivation also led to an obvious decrease in CBS protein levels in *Nrf1α*$^{-/-}$ or *Nrf2*$^{-/-}$ cells, when compared to its abundances measured from *WT* cells (Figures 5(m)–5(o) and S2, J-L).

Next, the effects of glucose deprivation on glutamate-cysteine ligase catalytic and modifier subunits (GCLC and GCLM, both comprising a key rate-limiting enzyme of glutathione biosynthesis) was investigated herein. As anticipated, both *GCLC* and *GCLM* mRNA expression was significantly induced by glucose deprivation of *WT* cells for 12 h (Figures 5(h) and 5(i)). Such induction of *GCLC* expression by glucose deprivation was completely abolished in *Nrf1α*$^{-/-}$ or *Nrf2*$^{-/-}$ cells, in which a considerable lower basal expression of *GCLC* was maintained by comparison with wild-type levels of HepG2 cells (Figure 5(h)). By contrast, basal and glucose starvation-stimulated *GCLM* expression levels were upregulated in *Nrf1α*$^{-/-}$ cells, but rather downregulated in *Nrf2*$^{-/-}$ cells (Figure 5(i)). However, *GCLC* and *GCLM* protein levels were almost unaffected after glucose starvation of the above examined three cell lines (Figures 5(m)–5(o) and S2, J-L).

Besides *GCLC* and *GCLM*, both *HO-1* (heme oxygenase 1, also called HMOX1) and *NQO1* (NAD(P)H quinone dehydrogenase 1) serve as downstream antioxidant genes of Nrf2 [36]. Here, an investigation by RT-qPCR revealed that glucose starvation for 12 h caused significant induction of *HO-1* and *NQO1* expression in *WT* cells (Figures 5(j) and 5(k)). By comparison, basal mRNA expression levels of *HO-1* and *NQO1* were upregulated in *Nrf1α*$^{-/-}$ cells, but rather downregulated in *Nrf2*$^{-/-}$ cells. Interestingly, remarkable induction of *HO-1*, rather than *NQO1*, by glucose deprivation was determined in *Nrf1α*$^{-/-}$ cells (Figures 5(j) and 5(k)). Conversely, transcriptional induction of *HO-1* and *NQO1* by glucose deprivation was roughly abolished or even slightly repressed in

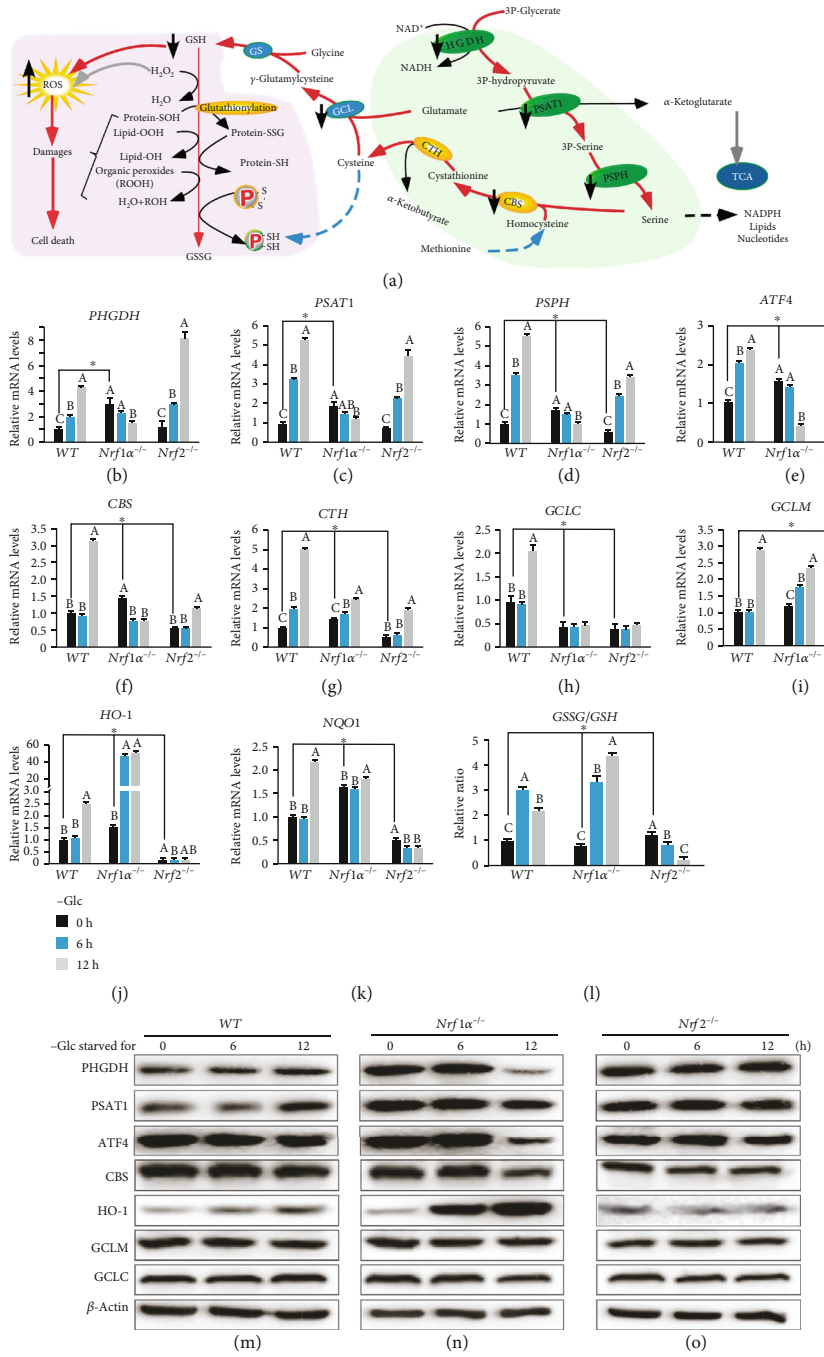


Figure 5: Fatal abolishment of *de novo* serine-to-glutathione biosynthesis by glucose deprivation of *Nrf1α*$^{-/-}$ cells. (a) A schematic to give a concise explanation of *de novo* serine synthesis pathway (SSP), along with ensuing transsulfuration to yield cysteine and glutathione (GSH). Both major buffers of GSH/GSSG and NADPH/NADP$^{+}$ are tightly regulated by redox cycling switches and relevant defense systems against ROS and oxidative damages. (b–k) Altered mRNA expression levels of key biosynthetic genes as follows: (i) (b) *PHGDH* (phosphoglycerate dehydrogenase), (c) *PSAT1* (phosphoserine aminotransferase 1), (d) *PSPH* (phosphoserine phosphatase) involved in the SSP, along with its regulator (e) *ATF4* (activating transcription factor 4); (ii) (f) *CBS* (cystathionine beta-synthase) and (g) *CTH* (cystathionine gamma-lyase) essential for the transsulfuration to yield cysteine; (iii) (h) *GCLC* (glutamate-cysteine ligase catalytic subunit) and (i) *GCLM* (glutamate-cysteine ligase modifier subunit) to catalyze glutathione biosynthesis; (iv) as well as antioxidant genes, such as (j) *HO-1* (heme oxygenase 1) and (k) *NQO1* (NAD(P)H quinone dehydrogenase 1), were determined by RT-qPCR of *WT*, *Nrf1α*$^{-/-}$, and *Nrf2*$^{-/-}$ cells that had been starved, or not starved, in the glucose-free media for 0-12 h. (l) Effects of glucose deprivation on the intracellular GSSG/GSH ratios in *WT*, *Nrf1α*$^{-/-}$, and *Nrf2*$^{-/-}$ cells were assessed. The asterisk "∗" only represents a significant change in *WT*, *Nrf1α*$^{-/-}$, and *Nrf2*$^{-/-}$ cell lines in the glucose-free culture for 0 h ($P < 0.05$), while the letters A, B, and C represent significant changes in the same cell line without glucose cultured for 0, 6, and 12 h ($P < 0.05$). (m–o) Changed abundances of PHGDH, PSAT1, ATF4, CBS, HO-1, GCLM, and GCLC proteins in *WT* (m), *Nrf1α*$^{-/-}$ (n), and *Nrf2*$^{-/-}$ (o) cells were visualized by Western blotting after glucose deprivation for 0-12 h.

*Nrf2*$^{-/-}$ cells. Furthermore, Western blotting showed that HO-1 protein abundances were significantly induced by glucose starvation of *WT* and *Nrf1α*$^{-/-}$ cells for 6-12 h but appeared to be completely abolished in *Nrf2*$^{-/-}$ cells (Figures 5(m)–5(o) and S2, J-L). Moreover, further examination unraveled that glucose deprivation caused a significant increase in the GSSG/GSH ratio in *WT* or *Nrf1α*$^{-/-}$ cells, but this ratio was reversely decreased in *Nrf2*$^{-/-}$ cells (Figure 5(l)). Together, these findings demonstrate that the death of *Nrf1α*$^{-/-}$ cells is a consequence of severe endogenous oxidative stress and damages induced by glucose starvation. This is attributable to fatal defects of *Nrf1α*$^{-/-}$ cells in the redox metabolic reprogramming, such that the intracellular GSH/GSSG imbalance is further deteriorated by glucose deprivation, even though certain antioxidant response genes are aberrantly activated by the hyperexpression of Nrf2 in *Nrf1α*-deficient cells.

*2.7. Distinct Requirements of Nrf1 and Nrf2 for the Redox Metabolic Reprogramming in Response to Glucose Deprivation.* To determine distinct roles of Nrf1 and Nrf2 in mediating cellular redox metabolic responses to glucose deprivation, we examined the expression of Nrf1 and Nrf2 *per se* after glucose starvation of different genotypic cells for 6-12 h. The RT-qPCR showed that the transcriptional expression of *Nrf1* and *Nrf2* was significantly induced by glucose deprivation in *WT* cells (Figures 6(a) and 6(b)). However, such inducible mRNA expression levels of *Nrf1* and *Nrf2* by glucose starvation, as well as their basal expression, were almost completely abolished in *Nrf1α*$^{-/-}$ and *Nrf2*$^{-/-}$ cells, respectively (Figures 6(a) and 6(b)). Interestingly, glucose starvation of *Nrf2*$^{-/-}$ cells for 12 h also caused a modest increase in *Nrf1* mRNA expression (Figure 6(a)), even though evident decreases in its basal mRNA levels (Figure 6(a)) and its Nrf1α-derived proteins (Figure 2(f)) were determined. Conversely, *Nrf1α*$^{-/-}$ cells only manifested a modest induction of *Nrf2* mRNA expression by glucose deprivation, but with no changes in its basal mRNA levels (Figure 6(b)), albeit its proteins were strikingly accumulated by loss of Nrf1α (Figure 2(f)). Collectively, these demonstrate the bidirectional interregulatory roles of between Nrf1 and Nrf2 in distinct contributions to the cellular response triggered by glucose deprivation, in which Nrf1α is a dominant player.

Intriguingly, Nrf1 and Nrf2 exhibited two different but similar trends in their protein levels. Glucose starvation of *WT* or *Nrf2*$^{-/-}$ cells stimulated conversion of Nrf1 glycoprotein-A and then proteolytic processing to yield mature cleaved protein-C/D isoforms before transcriptionally regulating target genes. Thereby, Figures 6(c) and 6(d) showed that glycoprotein-A of Nrf1 was gradually disappeared from 6 h to 12 h in glucose-starved *WT* or *Nrf2*$^{-/-}$ cells and then was replaced by gradual enhancement of active cleaved Nrf1 protein-C/D. By contrast, Nrf2 proteins in *WT* or *Nrf1α*$^{-/-}$ cells were marginally increased by glucose starvation for 6-12 h (Figures 6(e) and 6(f)). Such distinct abundances in both Nrf1 and Nrf2 proteins, together with both discrepant mRNA expression levels (Figures 6(a) and 6(b)), are attributable to their distinct stability and transactivity during glucose deprivation.

Given that Nrf1, but not Nrf2, exerts an essential biological role in transcriptional expression of proteasomes (PSM), we hence examined potential effects of glucose deprivation on Nrf1-target *PSM* genes, to gain a better understanding of disparate contributions of Nrf1 and Nrf2 to death of *Nrf1α*$^{-/-}$, but not *Nrf2*$^{-/-}$, cells suffered from glucose starvation. As anticipated, both mRNA and protein levels of *PSMB5*, *PSMB6*, and *PSMB7* (encoding the core enzymatic active β5, β1, and β2 subunits, respectively) were significantly abolished or suppressed in glucose-starved *Nrf1α*$^{-/-}$ cells, besides down-regulation of their basal expression levels to varying extents (Figures 6(e)–6(i)). Such being the case, all three core subunits *PSMB5*, *PSMB6*, and *PSMB7* in *WT* cells were also not induced by glucose deprivation. Reversely, mRNA expression of *PSMB5* in *WT* cells was significantly suppressed to less than 20% of its basal level during glucose starvation from 6 h to 12 h, but with no obvious changes in expression of *PSMB6* and *PSMB7* (Figures 6(g)–6(i)). Altogether, these demonstrate that negative regulation of proteasomal expression by glucose deprivation is much likely to result in the accumulation of oxidatively damaged proteins (including Nrf2), particularly in glucose-starved *Nrf1α*$^{-/-}$ cells.

To clarify distinct contributions of Nrf1 and Nrf2 to mediating cellular responses induced by glucose starvation, we determined conversion of these two CNC-bZIP proteins-derived isoforms and their stability during glucose deprivation as shown in Figure 6(j), time-course analysis revealed that the full-length Nrf1α glycoprotein-A was gradually converted into deglycoprotein-B, and ensuing processed protein-C/D in glucose-starved *WT* cells (of note, similar processing of Nrf1 had been interpreted in details, as elsewhere [37]). Consequently, Nrf1α glycoprotein-A and transient deglycoprotein-B became gradually fainter within 4 h of glucose starvation, while its protein-C/D abundances were conversely enhanced (Figure 6(k), left panel). All these Nrf1α-derived isoforms were accumulated by cotreatment with the proteasomal inhibitor bortezomib (BTZ) (Figures 6(j) and 6(k)). Furthermore, the stability of Nrf1 precursor protein-A/B and its mature processed protein-C/D in glucose-starved *WT* cells was estimated by their distinct half-lives, which were determined to be 0.24 h (=14.4 min) and 2.53 h (=151.8 min), respectively, after treatment with cycloheximide (CHX) (Figure S3). Of note, even in the presence of BTZ, glucose deprivation stimulated a rapid processing mechanism of Nrf1α glycoprotein-A and deglycoprotein-B (with a collective half-life of 0.41 h = 24.6 min) to yield certain amounts of its processed protein-C/D (with a more than 4-h half-life, Figures 6(j) and S3). By contrast, Nrf2 protein levels were almost unaffected by glucose starvation of *WT* cells, but their abundances were further enhanced by BTZ (Figures 6(j) and 6(k)). Moreover, Nrf2 protein stability under glucose deprivation conditions was determined by its half-life, which was estimated to be 0.42 h (=25.2 min) after CHX treatment, but also extended by BTZ to 1.10 h (=66 min) (Figure S3). Thereby, it is inferable that discrepant stability of Nrf1 and Nrf2 is dedicated to distinct roles of both CNC-bZIP factors in mediating disparate cellular responses to glucose starvation.

Next, to gain insights into direct roles of Nrf1 and Nrf2 in mediating key genes transcriptional responses required for redox metabolic reprogramming, we established 24 of the

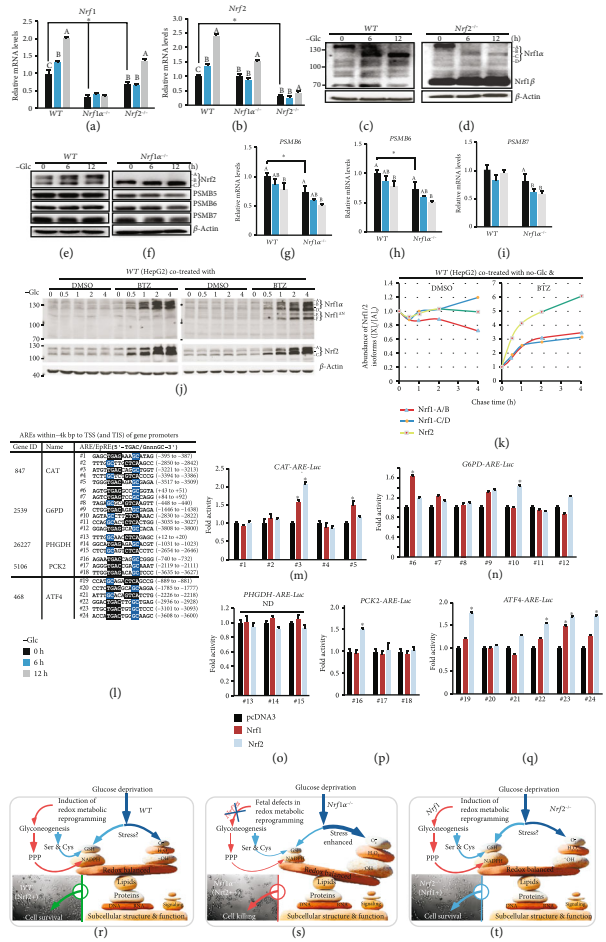

FIGURE 6: Distinct requirements of Nrf1 and Nrf2 for the cytoprotective response to glucose deprivation. (a, b) Distinct mRNA levels of *Nrf1* (*Nfe2l1*) (a) and *Nrf2* (*Nfe2l2*) (b) were determined by RT-qPCR analysis of *WT*, *Nrf1α*$^{-/-}$, and *Nrf2*$^{-/-}$ cells, which had been starved, or not starved, for 0-12 h in the glucose-free media. Then, the asterisk "∗" only represents a significant change in *WT*, *Nrf1α*$^{-/-}$, and *Nrf2*$^{-/-}$ cell lines in the glucose-free culture for 0 h ($P < 0.05$), while the letters A, B, and C represent significant changes in the same cell line without glucose cultured for 0, 6, and 12 h ($P < 0.05$). (c, d) Changes in Nrf1-derived protein isoforms in *WT* (c) and *Nrf2*$^{-/-}$ (d) cells were visualized by Western blotting after glucose deprivation for 0-12 h. (e, f) Western blotting of Nrf2, PSMB5, PSMB6, and PSMB7 proteins in *WT* (e) and *Nrf1α*$^{-/-}$ cells (f) was conducted after 0-12 h of glucose deprivation. (g–i) Alterations in mRNA levels of *PSMB5* (g), *PSMB6* (h), and *PSMB7* (i) in *WT* and *Nrf1α*$^{-/-}$ cells were determined after glucose starvation for 0-12 h. the asterisk "∗" only represents a significant change in *WT* and *Nrf1α*$^{-/-}$ cell lines in the glucose-free culture for 0 h ($P < 0.05$), while the letters A, B, and C represent significant changes in the same cell line without glucose cultured for 0, 6, and 12 h ($P < 0.05$). (j) *WT* cells were or were co-treated for 0-4 h in the glucose-free media containing 1 $\mu$mol/L bortezomib (BTZ, a proteasomal inhibitor) or 0.1% DMSO vehicle, followed by Western blotting with antibodies against Nrf1 or Nrf2. (k) The intensity of the immunoblots representing distinct Nrf1-derived isoforms or Nrf2 proteins, respectively, in the above-treated *WT* cells (j) was quantified by the Quantity One 4.5.2 software, and then shown graphically. (l) 24 of the indicated ARE-adjoining sequences searched from the promoter regions of *CAT*, *G6PD*, *PHGDH*, *PCK2*, and *ATF4* were cloned into the pGL3-Promoter vector, and the resulting contrasts served as *ARE*-driven luciferase (*ARE-Luc*) reporter genes. (m-q) *WT* cells were cotransfected with each of the above indicated *ARE-Luc* or non-*ARE-Luc* (as a background control) plasmids, together with an expression construct for Nrf1, Nrf2, or empty pcDNA3.1 vector, then allowed for 24-h recovery before the luciferase activity measured. The results were calculated as a fold change (mean ± S.D., $n = 9$) of three independent experiments. Then, the asterisk "∗" represents a significant change induced by expression Nrf1 or Nrf2, relative to that obtained from the empty *pcDNA3.1* vector, in cotransfection with the same *ARE-Luc* ($P < 0.05$ and change folds >1.4). ND, nonsignificant difference. (r–t) Three distinct models are proposed to provide a better understanding of molecular basis for survival or death decisions made by glucose-starved *WT* (r), *Nrf1α*$^{-/-}$ (s), and *Nrf2*$^{-/-}$ (t) cells. In redox metabolic reprogramming caused by glucose deprivation, the glycosis was diminished or abolished, and thus replaced by increased glyconeogenesis. As a result, many of their intermediates are diverted to enter the PPP and serine-to-glutathione biosynthesis pathways, in order to yield certain amounts of GSH and NADPH. These two reducing agents enable cytoprotective adaptation to oxidative stress induced by glucose deprivation (r). However, rapid death of *Nrf1α*$^{-/-}$ cells results from its fatal defects in the redox metabolic reprogramming in cellular response to glucose starvation, as accompanied by severe oxidative stress and damage accumulation (s). Thereby, Nrf1 is reasonable as a dominant player in the key gene regulation of redox metabolic reprogramming caused by glucose deprivation. As a result, the existence of Nrf1 in *Nrf2*$^{-/-}$ cells can still endow their survival with its redox metabolic reprogramming in a rebalanced redox state (t).

indicated luciferase reporter genes driven by consensus ARE sequences from the *CAT*, *G6PD*, *PHGDH*, *PCK2*, and *ATF4* promoter regions (Figure 6(l)). These ARE-driven Luciferase reporter assays revealed that transcriptional expression of *CAT-ARE(#3)-Luc* and *ATF4-ARE(#23)-Luc* was significantly activated by Nrf1 and Nrf2 (Figures 6(m)–6(q)). By contrast, Nrf2 alone also enabled transactivation of *G6PD-ARE(#10)-Luc*, *PCK2-ARE(#16)-Luc* and *ATF4-ARE(#19*, *#22*, and *#24)-Luc* (Figures 6(m)–6(q)), while only expression of *CAT-ARE(#5)-Luc* was upregulated by Nrf1 (Figure 6(m)). However, expression of all three *PHGDH-ARE-Luc* reporters appeared to be unaffected by either Nrf1 or Nrf2 (Figure 6(o)). Curiously, we should also notice that it is not hard to understand such seemingly-contradictory discrepancies between transactivation of these *ARE*-driven reporter genes mediated by Nrf1 (and Nrf2) (Figures 6(l)–6(q)) and relative high expression levels of the corresponding genes *CAT* (Figure 3(b)), *G6PD* (Figure 4(h)), *PCK2* (Figure 4(k)), and *PHGDH* (Figure 5(b)) in *Nrf1α*$^{-/-}$ cells (albeit aberrant accumulation of Nrf2 being retained as shown in Figures 2(f)–2(h)), when compared with their controls.

## 3. Discussion

In the previous study, we reported that knockout of *Nrf1α* leads to malignant proliferation and tumor metastasis [25, 30]. Such malignant growth and proliferation of cancer cells are also dictated by nutrient availability [38], because they require large amounts of nutrients intake. On this basis, we herein discover that glucose starvation prevents the malignant proliferation and even causes a lot of cell death in Nrf1α-deficient hepatoma cells. This is fully consistent with the therapeutic strategy against cancer by its nutrients limiting [39].

It is, to our surprise, that glucose starvation leads to rapid cellular death of *Nrf1α*$^{-/-}$ cells within 12 h, albeit with aberrant accumulation of Nrf2 in this deficient cells, whereas *Nrf2*$^{-/-}$ cells manifest a strong resistance to the lethality of glucose deprivation, even though Nrf1 is downregulated. This finding demonstrates that both Nrf1 and Nrf2 may be disparately involved in setting the thresholds of distinct cellular patho-physiological (e.g., redox metabolic) responses. This notion is also supported by the evidence showing a small number of *WT* cell deaths after glucose starvation for 24 h. Further examinations of cell death induced by glucose deprivation reveal that it is different from classical caspase-activated apoptosis, necroptosis, ferroptosis, and autophagy. Notably, a similar phenomenon was also observed after glucose starvation of other cell lines [40]. Contrarily, it is inferable that abnormal survival of *Nrf1α*$^{-/-}$ cells are, in its malignant growth and proliferation state, maintained by a highly energy-consuming mechanism so as to require its ever-incrementing amounts of glucose and other nutrients. By contrast, the energy-consumption of *Nrf2*$^{-/-}$ cells could be reduced to a considerable lower level than that of *WT* cells. Thus, the putative demand for glucose is positively correlated with the subcutaneous tumorigenicity of distinct cancer xenografts in nude mice, as reported by Qiu et al. [30]. Indeed, this is also corroborated by the previous finding that glucose uptake is substantially increased by silencing of *Nrf1* in pancreatic islet β-cells [29].

Further insights into acute death of glucose-starved *Nrf1α*$^{-/-}$ cells have unveiled that such a strong lethality should be ascribed to severe endogenous oxidative stress and damage accumulation. This notion is substantiated by several lines of experimental evidence as followed. Firstly, the accumulation of ROS in *Nrf1α*$^{-/-}$ cells, albeit with hyperactive Nrf2, is significantly augmented by glucose deprivation, as accompanied by depletion of GSH. These, together, result in a striking increment of the GSSG/GSH ratio during glucose starvation of *Nrf1α*$^{-/-}$ cells, in order to disrupt the intracellular redox balance and/or relevant signaling controls, as described by other groups [41, 42]. Secondly, the death of *Nrf1α*$^{-/-}$ cells induced by glucose starvation can be effectively prevented by both NAC and catalase, but not DHA. Similar results were obtained from the treatment of other cell lines with NAC and catalase to rescue its glucose starvation-induced death [43]. Thirdly, it is found that the GSSG/GSH ratio of *Nrf2*$^{-/-}$ cells is, conversely, diminished and even abolished during glucose starvation. Furtherly, silencing of Nrf2 in *Nrf1α*$^{-/-}$ cells can also enable them to be alleviated from the cytotoxic ROS accumulation, so that glucose starvation-induced death of *Nrf1α*$^{-/-}$ cells is sufficiently rescued by Nrf2 knockdown. Such surprising result implies that Nrf2 may also contribute to ROS production in *Nrf1α*$^{-/-}$ cells under basal and glucose deprivation conditions, albeit it has been accepted as a master regulator of antioxidant cytoprotective genes [44]. This is also supported by the finding that *Nrf1α*$^{-/-}$ cells are maintained at higher ROS levels in almost unstressed conditions, while *Nrf2*$^{-/-}$ cells are preserved at relatively lower ROS levels than those of *WT* cells (in this study). Similarly, a *de facto* contribution of Nrf2 to amplifying oxidative stress by upregulation of *KLF9* was reported by Zucker et al. [45]. Herein, our transcriptome sequencing revealed that *KLF9* expression level is too low to be detectable (Figure S4), but its family members *KLF4*, *KLF6*, *KLF10*, and *KLF13* are significantly upregulated by constitutive active Nrf2 (*caNrf2*). By contrast, only *KLF4*, *KLF5*, and *KLF16* were upregulated in *Nrf1α*$^{-/-}$ cells, but almost unaffected by *Nrf2*$^{-/-}$, whereas two paralogs SP1 and SP3 were partially increased in *Nrf2*$^{-/-}$ cells (Figure S4B), which await further study. Fourthly, glucose starvation-induced expression of *PSMB5*, *PSMB6*, and *PSMB7* (encoding the core subunits β5, β1, and β2) is substantially suppressed or even abolished in *Nrf1α*$^{-/-}$ cells (albeit retaining accumulation of Nrf2), besides their downregulated basal expression. Such proteasomal dysfunction is likely to contribute to the accumulation of oxidative damaged proteins (including Nrf2) to exacerbate endogenous oxidative stress in *Nrf1α*$^{-/-}$ cells. Taken together with our recent work [46], these lines of experimental evidence demonstrate that Nrf1 is more potent than Nrf2 at mediating intrinsic cytoprotective responses against cytotoxic effects of glucose deprivation, and other *bona fide* cellular stressors, such as tunicamycin alone or plus *tert*-butylhydroquinone.

In-depth insights into the endogenous molecular basis for oxidative stress, contributing to the lethality of glucose deprivation, unravel that dysfunctional redox defense

systems, along with altered redox signaling, are deteriorated in glucose-starved *Nrf1α*$^{-/-}$ cells. In fact, we found that, though a large amount of ROS accumulation leads to acute death in *Nrf1α*$^{-/-}$ cells, but conversely, a relatively low concentration of ROS is also accumulated, facilitating the maintenance of the malignant *Nrf1α*$^{-/-}$ cell growth and proliferation. This finding is in full agreement with the double-edged effects of ROS, acting as two distinct and even opposite players in cell growth, differentiation, progression, and death [47]. It is known that distinct high concentrations of ROS are involved in a variety of pathological processes, including cancer, ischemia, and immune and endocrine system deficiencies [47, 48]. The excessive ROS can also induce cell death by promoting the intrinsic apoptotic pathway [49]. Nonetheless, the low concentration of ROS is indispensable for various physiological processes, such as signal transduction and immune responses [48]. Such physiological ROS levels should be maintained in a steady-state by the homeostatic redox controls, including antioxidant defense systems, which comprise SOD, GPX1, GSR, CAT, and other redox proteins. As a result, the intracellular superoxide anions, arising from aggressive mitochondrial metabolism [50] and other sources (as illustrated in Figure 3(a)), are converted by SOD to $H_2O_2$ and oxygen, and then $H_2O_2$ is decomposed by CAT into water and oxygen [51, 52]. Furtherly, oxidized glutathione (GSSG) can be reduced by GSR to yield the sulfhydryl GSH [53]. GPX1 catalyzes the reduction of $H_2O_2$ and organic hydroperoxides by glutathione, so as to protect cells against oxidative damage [54]. In this study, we demonstrate that basal expression of *CAT* and *GPX1* is evidently upregulated in *Nrf1α*$^{-/-}$ cells (retaining hyper-active Nrf2 to activate the former consensus *ARE-luc* reporter), but substantially suppressed by glucose starvation. By contrast, basal expression of *GSR* and *SOD1* is obviously downregulated in *Nrf1α*$^{-/-}$ cells, and also further diminished by glucose deprivation. In addition, differential decreases of *TRX1*, *TRX2*, and *SOD2* occur only after glucose deprivation. Overall, dysfunctions of redox signaling controls and/or antioxidant defense systems are aggravated by glucose starvation of *Nrf1α*$^{-/-}$ cells, which contributes to the cellular lethality of this stress, albeit aberrant accumulation of hyperactive Nrf2. However, an exception to this is that NADPH oxidase 4 (NOX4), as a ROS-producing source, may also be coregulated by Nrf1 and Nrf2, based on the evidence that basal and starvation-stimulated expression of *NOX4* is significantly downregulated in *Nrf1α*$^{-/-}$ or *Nrf2*$^{-/-}$ cells. Besides, *CYBA* (also called *p22*$^{phox}$, which acts as a partner regulator of NADPH oxidases) was also decreased in *caNrf2* cells or *Nrf1α*$^{-/-}$ cells (with accumulated Nrf2), but unaltered in *Nrf2*$^{-/-}$ cells (Figure S4A). Yet, the detailed mechanism remains to be further explored in the future works.

To ameliorate the severe endogenous oxidative stress induced by glucose deprivation and thus facilitate survival and proliferation of cancer cells, they tend to redistribute those intermediates from both glycolysis and gluconeogenesis to other metabolic pathways (e.g., PPP and SSP, in Figures 4(a) and 5(a)). As stated by [55–57], the aerobic glycolysis, as a distinctive metabolic pattern of cancer cells from normal cells, provides a lot of intermediates for pentose phosphate pathway (PPP), gluconeogenesis and serine-to-glutathione synthesis pathway. Thus, this can enable cancer cells to reduce products of ROS from mitochondria and other subcellular compartments, but also enhance the generation of NADPH and GSH from PPP and glutathione synthesis, respectively, such that both NADPH/NADP$^+$ and GSH/GSSG ratio are restored to a newly redox-balanced level. However, we here found that such altered glucose metabolism pathways are dysregulated in *Nrf1α*$^{-/-}$ cells, and further deteriorated by glucose starvation, leading to the starved cell death. Among them mainly include increased glucose uptake, modestly reduced glycolysis, dysfunction of gluconeogenesis, PPP, and SSP. As a matter of fact, glucose deprivation results in an abject failure of glucose uptake and ensuing glycolysis. Thereby, this confers gluconeogenesis to gain the crucial importance, because gluconeogenesis is a potent alternative source of biosynthetic precursors under glucose deprivation, albeit its intermediates are shared from glycolytic pathways. Herein, we have proposed a conceptual model (as illustrated in Figure 6(r)–6(t)), based on the evidence that glucose starvation of *Nrf1α*$^{-/-}$ cells caused significant decreases in abundances of PCK2 and PCK1 (as key rate-limiting enzymes of gluconeogenesis), leading to an enhancement of the starved cell death, but similar results were not obtained from glucose-starved *WT* and *Nrf2*$^{-/-}$ cells. Conversely, *de facto* transcriptional expression of *PCK2* in *WT* or *Nrf2*$^{-/-}$ cells was strikingly activated by glucose deprivation. Similar upregulation of *PCK2* by low glucoses was also determined in A549 and H23 lung cancer cells, but its interference and inhibition also significantly enhanced their apoptosis induced by glucose deprivation [58]. This notion is further corroborated by another evidence showing that PCK2, but not PCK1, is highly expressed in different cancer cell lines [56, 59].

The resulting intermediates of gluconeogenesis in glucose-starved cancer cells are allowed for diversion to enter the PPP and serine-to-glutathione synthesis pathways, in order to restore the intracellular redox (e.g., NADPH/NADP$^+$ and GSH/GSSG) balances. Herein, we found that basal expression of *G6PD*, but not *PGD* (as two key enzymes to catalyze generation of NADPH), was upregulated in *Nrf1α*$^{-/-}$ cells, but glucose deprivation caused significant decreases of both expression in the exacerbated cellular death process. Similar decreased PPP flux, as accompanied by reduced NADPH levels and instead increased oxidative stress, was approved as a major fatal cause of the lethality of glucose starvation, because cell death was also accelerated by inhibiting G6PD [32]. However, it is full of curiosity that basal and glucose deprivation-stimulated expression levels of *G6PD* and *PGD* were substantially downregulated by *Nrf2*$^{-/-}$ cells to be considerably lower than those of *Nrf1α*$^{-/-}$ cells, but rather *Nrf2*$^{-/-}$ cells displayed a strong resistance to the lethality of glucose starvation. Such paradoxical observations indicate that other mechanisms, beyond PPP, are also involved in the response to glucose deprivation and its lethal cellular process. Thereby, distinct intracellular energy demands of ATP to determine cell survival or death decisions are also investigated, revealing that its basal ATP products are substantially augmented in *Nrf1α*$^{-/-}$ cells, but abruptly repressed by glucose

deprivation for 12 h to a much lower level than that of *WT* cells. By contrast, basal ATP levels of *Nrf2*$^{-/-}$ cells are markedly diminished to the lowest level, and also almost unaffected by glucose deprivation. Such disparate energy-consuming demands of between *Nrf1α*$^{-/-}$ and *Nrf2*$^{-/-}$ cell lines dictate their decision of survival or death, depending on gluconeogenesis and other nutrient sources in particular glucose deprivation conditions. In addition, we also discover that abundances of AMPK (as a key regulator of energy metabolism [34]) and phosphorylated AMPK$^{Thr172}$ (leading to its activation responsible for maintaining redox metabolic homeostasis [60]) are significantly suppressed by glucose starvation of *Nrf1α*$^{-/-}$ and *Nrf2*$^{-/-}$ cells, but with distinct (decreased or increased) ratios of phospho-AMPK$^{Thr172}$/AMPK. Altogether, the inactivation of AMPK to reduce ATP products is inferable as a main cause of blocking energy supply for glucose-starved *Nrf1α*$^{-/-}$ cells, which results in a large number of these cell deaths occurring after 12 h of glucose deprivation. In addition, it should be noted that this finding appears to be contradictory to two previous reports: one revealed that AMPK activation by glucose-starvation triggers autophagy of MEFs through phosphorylation of GAPDH at Ser122 and ensuing Sirt1 activation [61]; and the another showed that apoptotic death is promoted by AMPK activation in U2OS cells' response to glucose starvation [62]. Such discrepant results may be attributable to different experimental settings of different cell types with distinct responsive phenotypes to glucose deprivation.

Notably, serine biosynthesis is a vital turning point for glucose metabolism; its one hand provides an intermediate for anabolism, while its another hand directly affects cellular antioxidant capacity to generate cysteine and glutathione (as illustrated in Figure 5(a), [63, 64]). However, the effects of glucose limitation on serine-to-glutathione synthesis in cancer cells are, for the first time, determined here. From all this, we discovered that all key genes (i.e., *PHGDH*, *PSAT1*, *PSPH*, *CBS*, *CTH*, *GCLC*, and *GCLM*) for rate-limiting *de novo* serine-to-glutathione biosynthesis, along with *ATF4* (as a putative upstream regulator of serine synthesis [35]) and also two antioxidant genes (*HO-1* and *NQO1*), are substantially induced by glucose withdrawal from *WT* cells. Among them, basal expression levels of *PHGDH*, *PSAT1*, *PSPH*, and *CBS* were evidently upregulated in *Nrf1α*$^{-/-}$ cells, but unaffected or partially reduced by glucose deprivation. However, no significant changes in basal expression of these genes were observed in *Nrf2*$^{-/-}$ cells, but they were still induced by glucose starvation, as compared to those of *WT* cells. Such fatal defects of *Nrf1α*$^{-/-}$, but not *Nrf2*$^{-/-}$, cells in the serine biosynthesis and the ensuing transsulfuration to yield cysteine demonstrate that Nrf1*α* plays a dominant regulator in the successive processes. By contrast, Nrf2 is a master regulator of both GSH biosynthesis (*GCLC* and *GCLM*) and antioxidant responsive genes (*HO-1* and *NQO1*) to glucose deprivation, albeit Nrf1 is also involved in controlling *GCLC* expression.

## 4. Conclusion

In the present study, we found that glucose deprivation induces conversion of Nrf1 glycoprotein and then proteolytic processing to give rise to its mature cleaved CNC-bZIP factor, in order to transcriptionally regulate distinct target genes expression. Of note, Nrf1-target proteasomal expression is required for posttranslational processing of key proteins (e.g., Nrf2), but it is herein found that the core proteasomal subunits are inhibited by glucose deprivation. Under these conditions, gluconeogenesis becomes a major alternative source of biosynthetic precursors, and its intermediates are shared from glycolytic pathway and then diverted into other synthetic pathways (e.g., PPP and SSP). Thereby, altered glucose metabolism and energy demands of *Nrf1α*$^{-/-}$ cells are significantly aggravated by glucose deprivation, even though hyperactive Nrf2 is accumulated by loss of *Nrf1α*. Importantly, induction of serine-to-glutathione synthesis by glucose starvation is fatally abolished in *Nrf1α*$^{-/-}$ cells, leading to severe endogenous oxidative stress and relevant damage; this is even accompanied by upregulation of antioxidant responsive genes by Nrf2. Such fatal defects of *Nrf1α*$^{-/-}$, but not of *Nrf2*$^{-/-}$, cells in the redox metabolism reprogramming caused by glucose deprivation, lead rapidly to a large number of the former cell deaths, because the intracellular ROS are elevated, along with the reduced ATP production (Figures 6(r)–6(t)). Overall, these findings demonstrate that Nrf1 acts as a dominant player in the redox metabolic reprogramming and thus fulfill its intrinsic cytoprotective response against the fatal cytotoxicity of glucose deprivation. Thereby, the existence of Nrf1 still enables *Nrf2*$^{-/-}$ cells to be endowed with a strong constructive resistance to glucose starvation. Conversely, it is reasoned that Nrf2 cannot fulfill a fully cytoprotective function against severe oxidative stress and damage, although it serves as a master regulator of antioxidant response genes (e.g., *HO-1*, *NQO1*), which are still upregulated in *Nrf1α*$^{-/-}$ cells. Collectively, these demonstrate distinct contributions of Nrf1 and Nrf2 to either constructive or stress-inducible expression of different subsets of critical genes for the redox metabolism. Moreover, there exist certain interregulatory crosstalks between Nrf1 and Nrf2 in the redox metabolism reprogramming by coregulating expression of key responsive genes (e.g., *CAT*, *G6PD*, *PCK2*, *GCLC*, *ATF4*) to glucose deprivation.

## 5. Materials and Methods

*5.1. Cell Culture and Reagents.* The human hepatocellular carcinoma HepG2 cells (*WT*) were obtained originally from the American Type Culture Collection (ATCC, Manassas, VA, USA). The fidelity was conformed to be true by its authentication profiling and STR (short tandem repeat) typing map (by Shanghai Biowing Applied Biotechnology Co., Ltd). On this base, *Nrf1α*$^{-/-}$ and *Nrf2*$^{-/-}$ (or *Nrf2*$^{-/-\Delta TA}$) were established by Qiu et al. [30]. Before experimentation, they were maintained in Dulbecco's modified Eagle's medium (DMEM) containing 25 mmol/L high glucose, 10% (*v*/*v*) fetal bovine serum (FBS), 100 units/ml penicillin-streptomycin, and cultured in a 37°C incubator with 5% $CO_2$. In addition, it is noted that all key reagents and resources used in this study were listed in Table S1.

*5.2. Assays of Cell Death from Glucose Deprivation.* Equal numbers (300,000 or $3 \times 10^5$) of *WT*, *Nrf1α*$^{-/-}$ and *Nrf2*$^{-/-}$

cells were seeded in 6-well plates and allowed for growth in DMEM containing 25 mmol/L glucose and 10% FBS for 24 h. After reaching 80% of their confluence, they were then transferred to be cultured in fresh glucose-free DMEM for 6-24 h. Subsequently, the cell morphological changes in survival or death induced by glucose deprivation were observed by microscopy. These cells were then counted, after staining by trypan blue. In addition, *Nrf1α*$^{-/-}$*+siNrf2* cells were also prepared here, and then subjected to the cell death assay, after they were allowed for glucose deprivation.

To rescue the cell death, fructose and mannose (25 mmol/L) were added to the glucose-free media, respectively. The addition of 2DG (10 mmol/L) was to restore the PPP in the absence of glucose. In order to identify distinct types of cell death, q-VD-OPH (10 $\mu$mol/L, as a pan-caspase inhibitor), Necrostatin-1 (100 $\mu$mol/L), Ferrostatin-1 (2 $\mu$mol/L), and 3-methyladenine (2 mmol/L, an autophagy inhibitor) were added to the glucose-free media, respectively. Furthermore, NAC (5-10 mmol/L), CAT (50 units/ml), and DHA (100 $\mu$mol/L) were added in the glucose-free media to examine effects of antioxidants or prooxidants on cell death. After being incubated for 12-24 h, these cell morphological changes were visualized by microscopy, and the trypan-stained cells were also counted.

*5.3. Analysis of Cell Apoptosis and ROS by Flow Cytometry.* Equal numbers ($300,000$ or $3 \times 10^5$) of experimental cells (*WT*, *Nrf1α*$^{-/-}$, *Nrf2*$^{-/-}$, and *Nrf1α*$^{-/-}$*+siNrf2*) were allowed for 24 h of growth in DMEM containing 25 mmol/L glucose and 10% FBS for. After reaching 80% of their confluence, these cells were subjected to glucose deprivation by being cultured in a fresh glucose-free medium for 12 h. Subsequently, these cells were incubated with Annexin V-FITC and propidium iodide (PI) for 15 min, before the cell apoptosis was analyzed by flow cytometry. Furtherly, the intracellular ROS levels were also determined, according to the instruction of ROS assay kit (Beyotime, Shanghai, China). The resulting data were further analyzed by the FlowJo 7.6.1 software.

*5.4. Assays of ATP Levels and GSSG/GSH Ratios.* ATP levels are determined according to the instruction of enhanced ATP assay kit (Beyotime, Shanghai, China); GSSG/GSH ratios are determined according to the instruction of GSH and GSSG Assay Kit (Beyotime, Shanghai, China).

*5.5. Knockdown of Nrf2 in Nrf1α*$^{-/-}$ *Cells by Its siRNAs.* A pair of double-stranded small RNAs targeting for the interference with *Nrf2* (i.e., siNrf2) were synthesized by TranSheep Bio Co.Ltd. (Shanghai, China). The oligonucleotide sequences are as follows: FW, 5′-GUAAGAAGCCAGAUGU UAAdTdT-3′; REV, 5′-UUAACAUCUGGCUUCUUA CdTdT-3′. Subsequently, *Nrf1α*$^{-/-}$ cells were transfected with 80 nmol/L of the *siNrf2* oligonucleotides in the mixture of Lipofectamine 3000 (Invitrogen, California, USA). Thereafter, the *siNrf2*-interfered cells were identified by RT-qPCR and Western blotting, before being experimented.

*5.6. Real-Time Quantitative PCR Analysis of Gene Expression.* After all experimental cells reached 80% of their confluence, they were subjected to glucose starvation by being transferred in fresh glucose-free media. Their total RNAs were extracted after glucose deprivation for 0-12 h, before being subjected to the reactions with a reverse transcriptase to synthesize the first strand of cDNAs. Subsequently, the mRNA levels of examined genes in different cell lines were determined by RT-qPCR with the indicated pairs of their forward and reverse primers (as listed in Table S1). All the RT-qPCRs were carried out in the GoTaq real-time PCR detection systems by a CFX96 instrument (Bio-rad, Hercules, CA, USA). The resulting data were analyzed by the Bio-Rad CFX Manager 3.1 software (Bio-rad).

*5.7. Western Blotting Analysis of Key Functional Proteins.* After all experimental cells reached 80% of their confluence, they were subjected to glucose starvation by being transferred in fresh glucose-free media. After 6-12 h of glucose deprivation, their total proteins were extracted by lysis buffer (0.5% SDS, 0.04 mol/L DTT, pH 7.5) containing protease inhibitor cOmplete Tablets EASYpack or phosphatase inhibitor PhosSTOP EASYpack (each 1 tablet per 15 mL, Roche, Basel, Switzerland), and diluted in 6×SDS-PAGE sample loading buffer (Beyotime, Shanghai, China). Subsequently, total lysates were denatured immediately at 100°C for 10 min, before equal amounts of proteins were separated by SDS-PAGE gels containing 8-12% polyacrylamide and visualized by Western blotting with distinct primary antibodies (as listed in Table S1). Among included those antibodies against Nrf1; Nrf2, ATF4, GLUT1, GPX1, TRX1, TRX2, PRX1, CBS, HO1, GCLM, GCLC, GSR, SOD1, PCK1, PCK2 and G6PD, CAT, AMPK and p-AMPK$^{Thr172}$, PHGDH, PSAT1, HK1, HK2, PSMB5, PSMB6, and PSMB7. In addition, $\beta$-Actin served as an internal control to verify the amounts of proteins that were loaded in each of the wells.

*5.8. Assays of ARE-Driven Luciferase Reporter Gene Activity.* The core ARE consensus sites within -4K-bp sequences to the transcription start sites (TSS) or extended to the translation initiation sites (TIS) of *ATF4*, *CAT*, *G6PD*, *PHGDH*, and *PCK2* promoter regions were searched. Each of the core ARE and adjoining sequences was then inserted into the indicated site of the pGL3-promoter vector. The fidelity of all resultant constructs was confirmed by sequencing with indicated primer pairs (Table S1). Subsequently, equal numbers ($150,000$ or $1.5 \times 10^5$) of HepG2 cells were seeded in 12-well plates and allowed for 24-h growth in DMEM containing 25 mmol/L glucose and 10% FBS. After reaching 80% confluence, the cells were transfected with an expression construct for human Nrf1 or Nrf2, along with each of the above *ARE-Luc* reporters plus pRL-TK (serves as an internal control). Approximately 24 hours after transfection, ARE-driven luciferase activity was measured by using the dual-luciferase reporter assay. The resulting data were calculated as fold changes (mean ± S.D., $n = 9$), relative to the basal activity (at a given value of 1.0) obtained from the transfection of cells with an empty pcDNA3.1 and each of ARE-driven reporter genes.

*5.9. Statistical Analysis.* Statistical significance was assessed by using the ANOVA with Holm-Sidak test. The data presented herein are shown as a fold change (mean ± S.D., $n = 9$), each of which represents at least three independent experiments, that were each performed in triplicate.

## Data Availability

All the data needed to evaluate the findings of this study are available in this publication along with the "Supplemental Information" that can be found online. Additional other data related to this paper may also be requested from the corresponding author (with a lead contact at the email: yiguozhang@cqu.edu.cn, or eaglezhang64@gmail.com).

## Conflicts of Interest

The authors declare no conflict of interest. Besides, it should also be noted that the preprinted version of this paper had been initially posted at doi: 10.1101/2019.12.13.875369.

## Authors' Contributions

Y.-P.Z. performed the most experiments with the help of Z.Z. and collected relative data, except that Y.X. did the experimental analysis of the half-lives of Nrf1 and Nrf2. Y.-P.Z. also made a draft of this manuscript with most figures and supplemental tables. Y.Z. designed and supervised this study, analyzed all the data, helped to prepare all figures with cartoons, and wrote and revised the paper.

## Acknowledgments

We are greatly thankful to Drs. Lu Qiu (at Zhengzhou University, China) and Yonggang Ren (North Sichuan Medical College, Sichuan, China) for having established those relevant cell lines used in this study. We also thank Mr. Shaofan Hu and other members (at Chongqing University, China) for giving invaluable help with this work. Of note, the study was supported by the National Natural Science Foundation of China (NSFC, with a key program 91429305 and another project 81872336) awarded to Yiguo Zhang (at Chongqing University, China). This work is, in part, funded by Sichuan Department of Science and Technology grant (2019YJ0482) to Dr. Yuancai Xiang (at Southwest Medical University, Sichuan, China).

## Supplementary Materials

Figure S1: distinct cellular responses to glucose deprivation. Figure S2: the quantified results of western blot data in Figures 3, 4, and 5 by Quantity One 4.5.2 software. Figure S3: time-dependent effects of glucose deprivation on Nrf1 and Nrf2 with distinct half-lives. Figure S4: the mRNA expression of CYBA, NOXO1, and RAC1 in WT, Nrf1a-/-, Nrf1a-/- + siNrf2, Nrf2-/-, and caNrf2 from transcriptomic sequencing. Table S1: the key resources used in this work. *(Supplementary materials)*

## References

[1] D. Hanahan and R. A. Weinberg, "Hallmarks of cancer: the next generation," *Cell*, vol. 144, no. 5, pp. 646–674, 2011.

[2] Z. Li and H. Zhang, "Reprogramming of glucose, fatty acid and amino acid metabolism for cancer progression," *Cellular and Molecular Life Sciences*, vol. 73, no. 2, pp. 377–392, 2016.

[3] S. Y. Lunt and M. G. Vander Heiden, "Aerobic glycolysis: meeting the metabolic requirements of cell proliferation," *Annual Review of Cell and Developmental Biology*, vol. 27, no. 1, pp. 441–464, 2011.

[4] N. Hay, "Reprogramming glucose metabolism in cancer: can it be exploited for cancer therapy?," *Nature Reviews. Cancer*, vol. 16, no. 10, pp. 635–649, 2016.

[5] N. N. Pavlova and C. B. Thompson, "The emerging hallmarks of cancer metabolism," *Cell Metabolism*, vol. 23, no. 1, pp. 27–47, 2016.

[6] O. Warburg, "On the origin of cancer cells," *Science*, vol. 123, no. 3191, pp. 3309–3314, 1956.

[7] C. Munoz-Pinedo, N. El Mjiyad, and J. E. Ricci, "Cancer metabolism: current perspectives and future directions," *Cell Death & Disease*, vol. 3, no. 1, article e248, 2012.

[8] D. Xu, J. Jin, H. Yu et al., "Chrysin inhibited tumor glycolysis and induced apoptosis in hepatocellular carcinoma by targeting hexokinase-2," *Journal of Experimental & Clinical Cancer Research*, vol. 36, no. 1, p. 44, 2017.

[9] M. G. Vander Heiden, D. R. Plas, J. C. Rathmell, C. J. Fox, M. H. Harris, and C. B. Thompson, "Growth factors can influence cell growth and survival through effects on glucose metabolism," *Molecular and Cellular Biology*, vol. 21, no. 17, pp. 5899–5912, 2001.

[10] H.-C. Lee, S.-C. Lin, M.-H. Wu, and S.-J. Tsai, "Induction of pyruvate dehydrogenase kinase 1 by hypoxia alters cellular metabolism and inhibits apoptosis in endometriotic stromal cells," *Reproductive Sciences*, vol. 26, no. 6, pp. 734–744, 2018.

[11] A. Y. Choo, S. G. Kim, M. G. Vander Heiden et al., "Glucose addiction of TSC null cells is caused by failed mTORC1-dependent balancing of metabolic demand with supply," *Molecular Cell*, vol. 38, no. 4, pp. 487–499, 2010.

[12] N. El Mjiyad, A. Caro-Maldonado, S. Ramirez-Peinado, and C. Munoz-Pinedo, "Sugar-free approaches to cancer cell killing," *Oncogene*, vol. 30, no. 3, pp. 253–264, 2011.

[13] T. Mikawa, M. E. LLeonart, A. Takaori-Kondo, N. Inagaki, M. Yokode, and H. Kondoh, "Dysregulated glycolysis as an oncogenic event," *Cellular and Molecular Life Sciences*, vol. 72, no. 10, pp. 1881–1892, 2015.

[14] L. Sun, L. Song, Q. Wan et al., "cMyc-mediated activation of serine biosynthesis pathway is critical for cancer progression under nutrient deprivation conditions," *Cell Research*, vol. 25, no. 4, pp. 429–444, 2015.

[15] D. Huang, C. Li, and H. Zhang, "Hypoxia and cancer cell metabolism," *Acta Biochimica et Biophysica Sinica*, vol. 46, no. 3, pp. 214–219, 2014.

[16] J. W. Kim, I. Tchernyshyov, G. L. Semenza, and C. V. Dang, "HIF-1-mediated expression of pyruvate dehydrogenase kinase: a metabolic switch required for cellular adaptation to hypoxia," *Cell Metabolism*, vol. 3, no. 3, pp. 177–185, 2006.

[17] F. Schwartzenberg-Bar-Yoseph, M. Armoni, and E. Karnieli, "The tumor suppressor p53 down-regulates glucose transporters GLUT1 and GLUT4 gene expression," *Cancer Research*, vol. 64, no. 7, pp. 2627–2633, 2004.

[18] Y. Zhang and Y. Xiang, "Molecular and cellular basis for the unique functioning of Nrf1, an indispensable transcription factor for maintaining cell homoeostasis and organ integrity," *The Biochemical Journal*, vol. 473, no. 8, pp. 961–1000, 2016.

[19] H. Satoh, T. Moriguchi, J. Takai, M. Ebina, and M. Yamamoto, "Nrf2 prevents initiation but accelerates progression through the Kras signaling pathway during lung carcinogenesis," *Cancer Research*, vol. 73, no. 13, pp. 4158–4168, 2013.

[20] S. Tao, M. Rojo de la Vega, E. Chapman, A. Ooi, and D. D. Zhang, "The effects of NRF2 modulation on the initiation and progression of chemically and genetically induced lung cancer," *Molecular Carcinogenesis*, vol. 57, no. 2, pp. 182–192, 2018.

[21] H. Wang, X. Liu, M. Long et al., "NRF2 activation by antioxidant antidiabetic agents accelerates tumor metastasis," *Science Translational Medicine*, vol. 8, no. 334, article 334ra51, 2016.

[22] Y. Y. Wang, J. Chen, X. M. Liu, R. Zhao, and H. Zhe, "Nrf2-mediated metabolic reprogramming in cancer," *Oxidative Medicine and Cellular Longevity*, vol. 2018, 7 pages, 2018.

[23] J. D. Hayes and A. T. Dinkova-Kostova, "The Nrf2 regulatory network provides an interface between redox and intermediary metabolism," *Trends in Biochemical Sciences*, vol. 39, no. 4, pp. 199–218, 2014.

[24] Y. Zhang, S. Li, Y. Xiang, L. Qiu, H. Zhao, and J. D. Hayes, "The selective post-translational processing of transcription factor Nrf1 yields distinct isoforms that dictate its ability to differentially regulate gene expression," *Scientific Reports*, vol. 5, no. 1, 2015.

[25] Y. Ren, L. Qiu, F. Lu et al., "TALENs-directed knockout of the full-length transcription factor Nrf1$\alpha$ that represses malignant behaviour of human hepatocellular carcinoma (HepG2) cells," *Scientific Reports*, vol. 6, no. 1, 2016.

[26] Y. Hirotsu, N. Hataya, F. Katsuoka, and M. Yamamoto, "NF-E2-related factor 1 (Nrf1) serves as a novel regulator of hepatic lipid metabolism through regulation of the Lipin1 and PGC-1beta genes," *Molecular and Cellular Biology*, vol. 32, no. 14, pp. 2760–2770, 2012.

[27] T. Tsujita, V. Peirce, L. Baird et al., "Transcription factor Nrf1 negatively regulates the cystine/glutamate transporter and lipid-metabolizing enzymes," *Molecular and Cellular Biology*, vol. 34, no. 20, pp. 3800–3816, 2014.

[28] Y. Hirotsu, C. Higashi, T. Fukutomi et al., "Transcription factor NF-E2-related factor 1 impairs glucose metabolism in mice," *Genes to Cells*, vol. 19, no. 8, pp. 650–665, 2014.

[29] H. Zheng, J. Fu, P. Xue et al., "CNC-bZIP protein Nrf1-dependent regulation of glucose-stimulated insulin secretion," *Antioxidants & Redox Signaling*, vol. 22, no. 10, pp. 819–831, 2015.

[30] L. Qiu, M. Wang, S. Hu et al., "Oncogenic activation of Nrf2, though as a master antioxidant transcription factor, liberated by specific knockout of the full-length Nrf1$\alpha$ that acts as a dominant tumor repressor," *Cancers*, vol. 10, no. 12, p. 520, 2018.

[31] E. Perales-Clemente, C. D. L. Folmes, and A. Terzic, "Metabolic regulation of redox status in stem cells," *Antioxidants & Redox Signaling*, vol. 21, no. 11, pp. 1648–1659, 2014.

[32] S. M. Jeon, N. S. Chandel, and N. Hay, "AMPK regulates NADPH homeostasis to promote tumour cell survival during energy stress," *Nature*, vol. 485, no. 7400, pp. 661–665, 2012.

[33] Y. Zhang, D. H. Crouch, M. Yamamoto, and J. D. Hayes, "Negative regulation of the Nrf1 transcription factor by its N-terminal domain is independent of Keap1: Nrf1, but not Nrf2, is targeted to the endoplasmic reticulum," *The Biochemical Journal*, vol. 399, no. 3, pp. 373–385, 2006.

[34] D. G. Hardie, B. E. Schaffer, and A. Brunet, "AMPK: an energy-sensing pathway with multiple inputs and outputs," *Trends in Cell Biology*, vol. 26, no. 3, pp. 190–201, 2016.

[35] E. Zhao, J. Ding, Y. Xia et al., "KDM4C and ATF4 cooperate in transcriptional control of amino acid metabolism," *Cell Reports*, vol. 14, no. 3, pp. 506–519, 2016.

[36] L. B. Nam and Y. S. Keum, "Binding partners of NRF2: functions and regulatory mechanisms," *Archives of Biochemistry and Biophysics*, vol. 678, article 108184, 2019.

[37] Y. Xiang, M. Wang, S. Hu et al., "Mechanisms controlling the multistage post-translational processing of endogenous Nrf1$\alpha$/TCF11 proteins to yield distinct isoforms within the coupled positive and negative feedback circuits," *Toxicology and Applied Pharmacology*, vol. 360, pp. 212–235, 2018.

[38] M. G. Vander Heiden and R. J. DeBerardinis, "Understanding the intersections between metabolism and cancer biology," *Cell*, vol. 168, no. 4, pp. 657–669, 2017.

[39] M. R. Sullivan and M. G. Vander Heiden, "Determinants of nutrient limitation in cancer," *Critical Reviews in Biochemistry and Molecular Biology*, vol. 54, no. 3, pp. 193–207, 2019.

[40] C. L. Leon-Annicchiarico, S. Ramirez-Peinado, D. Dominguez-Villanueva, A. Gonsberg, T. J. Lampidis, and C. Munoz-Pinedo, "ATF4 mediates necrosis induced by glucose deprivation and apoptosis induced by 2-deoxyglucose in the same cells," *The FEBS Journal*, vol. 282, no. 18, pp. 3647–3658, 2015.

[41] V. Nogueira and N. Hay, "Molecular pathways: reactive oxygen species homeostasis in cancer cells and implications for cancer therapy," *Clinical Cancer Research*, vol. 19, no. 16, pp. 4309–4314, 2013.

[42] Y. Liu, X. D. Song, W. Liu, T. Y. Zhang, and J. Zuo, "Glucose deprivation induces mitochondrial dysfunction and oxidative stress in PC12 cell line," *Journal of Cellular and Molecular Medicine*, vol. 7, no. 1, pp. 49–56, 2003.

[43] P. Gonzalez-Menendez, D. Hevia, R. Alonso-Arias et al., "GLUT1 protects prostate cancer cells from glucose deprivation-induced oxidative stress," *Redox Biology*, vol. 17, pp. 112–127, 2018.

[44] A.-A. Zimta, D. Cenariu, A. Irimie et al., "The role of Nrf2 activity in cancer development and progression," *Cancers*, vol. 11, no. 11, p. 1755, 2019.

[45] S. N. Zucker, E. E. Fink, A. Bagati et al., "Nrf2 amplifies oxidative stress via induction of Klf9," *Molecular Cell*, vol. 53, no. 6, pp. 916–928, 2014.

[46] Y. P. Zhu, Z. Zheng, S. Hu et al., "Unification of opposites between two antioxidant transcription factors Nrf1 and Nrf2 in mediating distinct cellular responses to the endoplasmic reticulum stressor tunicamycin," *Antioxidants*, vol. 9, no. 1, p. 4, 2020.

[47] J. É. M. MatÉs, C. Pérez-Gómez, and I. N. De Castro, "Antioxidant enzymes and human diseases," *Clinical Biochemistry*, vol. 32, no. 8, pp. 595–603, 1999.

[48] V. Monnier, F. Girardot, W. Audin, and H. Tricoire, "Control of oxidative stress resistance by IP3 kinase in Drosophila melanogaster," *Free Radical Biology & Medicine*, vol. 33, no. 9, pp. 1250–1259, 2002.

[49] S. Marchi, C. Giorgi, J. M. Suski et al., "Mitochondria-ros crosstalk in the control of cell death and aging," *Journal of Signal Transduction*, vol. 2012, 17 pages, 2012.

[50] S. H. Chang, J. Garcia, J. A. Melendez, M. S. Kilberg, and A. Agarwal, "Haem oxygenase 1 gene induction by glucose deprivation is mediated by reactive oxygen species via the mitochondrial electron-transport chain," *The Biochemical Journal*, vol. 371, no. 3, pp. 877–885, 2003.

[51] C. Michiels, M. Raes, O. Toussaint, and J. Remacle, "Importance of se-glutathione peroxidase, catalase, and Cu/Zn-SOD for cell survival against oxidative stress," *Free Radical Biology & Medicine*, vol. 17, no. 3, pp. 235–248, 1994.

[52] H. Aebi, "[13] Catalase in vitro," *Methods in Enzymology*, vol. 105, pp. 121–126, 1984.

[53] P. Pyne, M. Alam, and W. Ghosh, "A novel soxO gene, encoding a glutathione disulfide reductase, is essential for tetrathionate oxidation in Advenella kashmirensis," *Microbiological Research*, vol. 205, pp. 1–7, 2017.

[54] E. Lubos, J. Loscalzo, and D. E. Handy, "Glutathione peroxidase-1 in health and disease: from molecular mechanisms to therapeutic opportunities," *Antioxidants & Redox Signaling*, vol. 15, no. 7, pp. 1957–1997, 2011.

[55] K. C. Patra and N. Hay, "The pentose phosphate pathway and cancer," *Trends in Biochemical Sciences*, vol. 39, no. 8, pp. 347–354, 2014.

[56] E. . E. Vincent, A. Sergushichev, T. Griss et al., "Mitochondrial phosphoenolpyruvate carboxykinase regulates metabolic adaptation and enables glucose-independent tumor growth," *Molecular Cell*, vol. 60, no. 2, pp. 195–207, 2015.

[57] J. W. Locasale, "Serine, glycine and one-carbon units: cancer metabolism in full circle," *Nature Reviews. Cancer*, vol. 13, no. 8, pp. 572–583, 2013.

[58] K. Leithner, A. Hrzenjak, M. Trotzmuller et al., "PCK2 activation mediates an adaptive response to glucose depletion in lung cancer," *Oncogene*, vol. 34, no. 8, pp. 1044–1050, 2015.

[59] A. Mendez-Lucas, P. Hyrossova, L. Novellasdemunt, F. Vinals, and J. C. Perales, "Mitochondrial phosphoenolpyruvate carboxykinase (PEPCK-M) is a pro-survival, endoplasmic reticulum (ER) stress response gene involved in tumor cell adaptation to nutrient availability," *The Journal of Biological Chemistry*, vol. 289, no. 32, pp. 22090–22102, 2014.

[60] Y. Ren and H. M. Shen, "Critical role of AMPK in redox regulation under glucose starvation," *Redox Biology*, vol. 25, article 101154, 2019.

[61] C. Chang, H. Su, D. Zhang et al., "AMPK-dependent phosphorylation of GAPDH triggers Sirt1 activation and is necessary for autophagy upon glucose starvation," *Molecular Cell*, vol. 60, no. 6, pp. 930–940, 2015.

[62] R. Okoshi, T. Ozaki, H. Yamamoto et al., "Activation of AMP-activated protein kinase induces p53-dependent apoptotic cell death in response to energetic stress," *The Journal of Biological Chemistry*, vol. 283, no. 7, pp. 3979–3987, 2008.

[63] S. C. Kalhan and R. W. Hanson, "Resurgence of serine: an often neglected but indispensable amino acid," *The Journal of Biological Chemistry*, vol. 287, no. 24, pp. 19786–19791, 2012.

[64] I. Amelio, F. Cutruzzola, A. Antonov, M. Agostini, and G. Melino, "Serine and glycine metabolism in cancer," *Trends in Biochemical Sciences*, vol. 39, no. 4, pp. 191–198, 2014.